PSFC/JA-06-1

Effects of Hot Electrons on the Stability of a Dipolar Plasma

Natalia S. Krasheninnikova and Peter J. Catto

February 2006

MIT Plasma Science and Fusion Center
Cambridge, MA 02139

This work was supported by the U.S. Department of Energy, Grant No. DE-FG02-91ER-54109.

Submitted for publication in the Physics of Plasmas

Effects of hot electrons on the stability of a dipolar plasma*

Natalia S. Krasheninnikova, Peter J. Catto

Massachusetts Institute of Technology, Plasma Science and Fusion Center

Cambridge, MA 02139

Abstract

We investigate the effects of a hot species on plasma stability in dipolar magnetic field. The results can be applied to the dipole experiments employing the electron cyclotron heating. We consider the interchange stability of a plasma of fluid background electrons and ions with a small fraction of hot kinetic electrons. The species diamagnetic drift and magnetic drift frequencies are assumed to be of the same order, and the wave frequency is assumed to be much larger than the background, but much less than the hot drift frequencies. We derive and analyze an arbitrary total pressure dispersion relation to obtain the general requirements for stability in dipolar geometry. As an application of the theory, we consider a special separable form of a point dipole equilibrium. Our analysis shows that a weak drift resonance with the slowly moving hot electrons modifies the simple Magnetohydrodynamic (MHD) interchange stability condition. Destabilization by this weak drift resonance can be avoided by carefully controlling the hot electron density and temperature profiles. A strong hot electron destabilization due to magnetic drift reversal is found not to occur in point dipole geometry.

* Research supported by US Dept. of Energy.

PACS numbers: 52.58.Lq, 52.55.Tn, 52.55.Hc.

I. INTRODUCTION

The Levitated Dipole Experiment (LDX)[1,2] has been built and operated in an MHD interchange stable regime[3-6]. The hot electron population is created by the electron cyclotron heating that increases the electron temperature[7] and can alter the interchange stability of plasma. We examine the role the hot electrons play in modifying the usual ideal MHD interchange stability condition including wave-particle resonance effects by considering a confined plasma with an ideal fluid background consisting of electrons and ions plus a fully kinetic population of hot electrons. Based on current LDX experimental observations, unstable modes with frequencies ranging from two to five of kHz to hundreds of MHz are being observed[8], corresponding to typical magnetic drift frequencies of the background species and hot electrons, respectively.

The format of this calculation is similar to that in our Z-pinch paper[9], but is applied here to general dipolar geometry for which the unperturbed magnetic field B_0 is purely in the poloidal direction, while the unperturbed diamagnetic current J_0 is toroidal. To concentrate on the role the hot electrons play in modifying the interchange stability, we only consider flute modes with wave frequencies much higher than the background and lower than the hot species drift frequencies, since they are the least stable modes in the absence of hot electrons[3-6]. As a result of our ordering, we do not consider the hot electron interchange, for which the mode frequency is of the order of the typical hot electron frequency, such as magnetic and diamagnetic. We treat the magnetic drift, consisting of comparable grad B_0 and curvature drifts, on equal footing with the diamagnetic drift. We obtain the dispersion relation for arbitrary plasma and hot electron pressures, but then examine three plasma pressure orderings relative to

the magnetic pressure: background electrostatic with $\beta_b << \beta_h \sim 1$, electromagnetic with $1 \sim \beta_b << \beta_h$, and electromagnetic with $1 \sim \beta_b \sim \beta_h$. Throughout the paper we compare and contrast the results from dipolar geometry to that of the Z-pinch.

In Sec. II we derive two coupled equations for the ideal MHD background plasma that involve the perturbed hot electron number density and the $\nabla\psi$ component of the current. These two quantities are then evaluated kinetically in Sec. III. Section IV combines the results from the two previous sections to obtain the full dispersion relation, and general stability conditions, including a discussion of hot electron drift resonance de-stabilization effects. As an application of the above theory, a separable form of a point dipole equilibrium is considered and the results obtained are presented in Sec. V. We close with a brief discussion of the analysis in Sec. VI.

II. IDEAL MHD TREATMENT OF THE BACKGROUND PLASMA

Our derivation for the dipole geometry will follow the guidelines developed for the Z-pinch[9]. In this section we will use an ideal MHD treatment to derive the $\nabla\psi$ component of the perturbed Ampere's law and a perturbed quasi-neutrality condition. The quantities pertaining to the hot species, such as $\nabla\psi$ component of the perturbed current and number density, will be evaluated kinetically in the next section.

Using the standard approach for the closed field line axisymmetric or dipole configuration we introduce poloidal magnetic flux ψ, toroidal angle ζ and radial distance from the axis of symmetry R so that the unperturbed poloidal magnetic field and toroidal current are given by:

$$\vec{\mathbf{B}}_0 = \nabla\psi \times \nabla\zeta \text{ and } \vec{\mathbf{J}}_0 = R^2 \frac{dp_0}{d\psi}\nabla\zeta \tag{1}$$

where the total pressure p_0, is the sum of the hot pressure p_{0h} and the background pressure $p_{0b} = n_{0e}T_e + n_{0i}T_i$, with n_{0e}, n_{0i}, T_e, and T_i the background electron and ion densities and temperatures, respectively. The total current is the sum of the background and hot contributions $J_0 = J_{0b} + J_{0h}$ which separately satisfy the force balance relations to give $\vec{\mathbf{J}}_{0b} = (dp_{0b}/d\psi)R^2\nabla\zeta$ and $\vec{\mathbf{J}}_{0h} = (dp_{0h}/d\psi)R^2\nabla\zeta$. Using the Ampere's law to derive the Grad-Shafranov equation yields

$$\nabla\cdot\left(\frac{\nabla\psi}{R^2}\right) + \mu_0\frac{dp_0}{d\psi} = 0\,.$$

Defining $\vec{\boldsymbol{\kappa}} = (\hat{\mathbf{b}}\cdot\nabla)\hat{\mathbf{b}}$ as magnetic field curvature with $\hat{\mathbf{b}} = \vec{\mathbf{B}}_0/B_0$, it also follows from the preceding equation and equilibrium pressure balance that

$$\frac{2\vec{\boldsymbol{\kappa}}\cdot\nabla\psi}{B_0^2R^2} = \frac{\beta_0}{2}\frac{d\ln p_0}{d\psi} - \nabla\cdot\left(\frac{\nabla\psi}{B_0^2R^2}\right), \tag{2}$$

where

$$\beta_0 \equiv \frac{2\mu_0 p_0}{B_0^2}\,.$$

We assume perturbations of the form $\hat{\mathbf{Q}}_1(\psi,\theta)e^{-i\omega t - il\zeta}$, with θ the poloidal angle and $\mathrm{Im}\,\omega > 0$ for instability. Then, we perturb around this equilibrium by introducing the displacement vector $\vec{\xi}$ as $\vec{\mathbf{v}}_1 = -i\omega\vec{\xi}$, with $\vec{\mathbf{v}}_1$ the background ion flow velocity, and writing it as

$$\vec{\xi} = \xi_B\frac{\vec{\mathbf{B}}_0}{B_0^2} + \xi_\psi\frac{\nabla\psi}{|\nabla\psi|^2} + \xi_\zeta\frac{\nabla\zeta}{|\nabla\zeta|^2}\,. \tag{3}$$

Using the usual ideal MHD equations, the perturbed electric field $\vec{\mathbf{E}}_1$, magnetic field $\vec{\mathbf{B}}_1$ and total current $\vec{\mathbf{J}}_1 = \vec{\mathbf{J}}_{1b} + \vec{\mathbf{J}}_{1h}$ are given by

$$\vec{\mathbf{E}}_1 = i\omega\vec{\boldsymbol{\xi}} \times \vec{\mathbf{B}}_0, \tag{4}$$

$$\vec{\mathbf{B}}_1 = \nabla \times \left(\vec{\boldsymbol{\xi}} \times \vec{\mathbf{B}}_0\right), \text{ and} \tag{5}$$

$$\mu_0 \vec{\mathbf{J}}_1 = \nabla \times \vec{\mathbf{B}}_1, \tag{6}$$

where it is convenient to write $\vec{\mathbf{B}}_1$ as

$$\vec{\mathbf{B}}_1 = Q_B \frac{\vec{\mathbf{B}}_0}{B_0^2} + Q_\psi \frac{\nabla\psi}{|\nabla\psi|^2} + Q_\zeta \frac{\nabla\zeta}{|\nabla\zeta|^2}. \tag{7}$$

Equations (3) and (5) give $Q_B = -B_0^2\left(\frac{\nabla\zeta\cdot\nabla\xi_\zeta}{|\nabla\zeta|^2} + \frac{\nabla\psi\cdot\nabla\xi_\psi}{|\nabla\psi|^2}\right)$, $Q_\psi = \vec{\mathbf{B}}_0 \cdot \nabla\xi_\psi$ and $Q_\zeta = \vec{\mathbf{B}}_0 \cdot \nabla\xi_\zeta$.

In addition, background plasma momentum and energy conservation are written as

$$-m_i n_{0i}\omega^2\vec{\boldsymbol{\xi}} = en_{0h}\vec{\mathbf{E}}_1 + \vec{\mathbf{J}}_{1b} \times \vec{\mathbf{B}}_0 + \vec{\mathbf{J}}_{0b} \times \vec{\mathbf{B}}_1 - \nabla p_{1b}, \tag{8}$$

and

$$p_{1b} = -\gamma p_{0b}\nabla\cdot\vec{\boldsymbol{\xi}} - \frac{dp_{0b}}{d\psi}\xi_\psi, \tag{9}$$

where m_i denotes the mass of the background ions, p_{1b} is perturbed background pressure, and $\gamma = 5/3$. The $\vec{\mathbf{E}}_1$ term in the momentum equation, which is absent in the usual ideal MHD treatment, enters due to the effect of charge uncovering – the incomplete shielding of the background electrons by the background ions since the equilibrium quasineutrality for singly charged ions requires $n_{0h} = n_{0i} - n_{0e}$.

Using the preceding system of equations, it is convenient to define

$$W = -p_{1b} - \xi_\psi \frac{dp_{0b}}{d\psi} = \gamma p_{0b}\nabla\cdot\vec{\boldsymbol{\xi}}, \tag{10}$$

and then obtain two coupled equations for W and ξ_ψ, both of which only require knowledge of the perturbed hot electron density and current, which are evaluated in the next section. To

simplify the procedure we use the parallel component of Faraday's law and Eq. (3) to form $\nabla\cdot\vec{\xi}$ and to obtain two convenient expressions for ξ_ζ and Q_B

$$il\xi_\zeta = \frac{\nabla\psi\cdot\nabla\xi_\psi}{|\nabla\psi|^2} + \frac{Q_B}{B_0^2}, \tag{11}$$

and

$$\frac{Q_B}{B_0^2} = \vec{\mathbf{B}}_0\cdot\nabla\left(\frac{\xi_B}{B_0^2}\right) + \xi_\psi\nabla\cdot\left(\frac{\nabla\psi}{|\nabla\psi|^2}\right) - \frac{W}{\gamma p_{0b}}. \tag{12}$$

Next, we consider the $\nabla\psi$ component of Ampere's law,

$$\mu_0\vec{\mathbf{J}}_1\cdot\nabla\psi = \mu_0\vec{\mathbf{J}}_{1b}\cdot\nabla\psi + \mu_0\vec{\mathbf{J}}_{1h}\cdot\nabla\psi = -ilQ_B - \vec{\mathbf{B}}_0\cdot\nabla\left(R^2Q_\zeta\right). \tag{13}$$

The background contribution is calculated from the toroidal component of the momentum equation yielding

$$\vec{\mathbf{J}}_{1b}\cdot\nabla\psi = m_i n_{0i}\omega^2R^2\xi_\zeta + en_{0h}R^2\vec{\mathbf{E}}_1\cdot\nabla\zeta + ilp_{1b},$$

with ξ_ζ given by Eq. (11), p_{1b} given by Eq. (10), and $\vec{\mathbf{E}}_1\cdot\nabla\zeta = -i\omega|\nabla\zeta|^2\xi_\psi$ from the toroidal component of Eq. (4). Defining the background plasma beta as

$$\beta_b \equiv \frac{2\mu_0 p_{0b}}{B_0^2},$$

and using Eq. (11), the $\nabla\psi$ component of Ampere's law can be rewritten as

$$\begin{aligned} &-\frac{\mu_0\vec{\mathbf{J}}_{1h}\cdot\nabla\psi}{ilB_0^2} - \frac{\vec{\mathbf{B}}_0\cdot\nabla\left(R^2Q_\zeta\right)}{ilB_0^2} + \frac{\beta_b W}{2p_{0b}} + \frac{1}{2}\beta_b\left(\frac{d\ln p_{0b}}{d\psi}\xi_\psi + \frac{\omega e n_{0h}}{l p_{0b}}\xi_\psi + \frac{m_i n_{0i}\omega^2R^2}{l^2 p_{0b}}\frac{\nabla\psi\cdot\nabla\xi_\psi}{|\nabla\psi|^2}\right) \\ &= \left(1-\beta_b\frac{m_i n_{0i}\omega^2R^2}{2l^2 p_{0b}}\right)\frac{Q_B}{B_0^2}. \end{aligned} \tag{14}$$

The most unstable ideal MHD ballooning-interchange modes have $l >> 1$ for an axisymmetric torus with closed field lines[3]. Therefore, we can use the standard high mode

number formalism to neglect the $1/l^2$ term from $\vec{\mathbf{B}}_0 \cdot \nabla\left(R^2 Q_\zeta\right)$ and the coupling to the magnetosonic waves by assuming $\omega^2 R^2 / l^2 << p_{0b} / m_i n_{0i}$ in Eq. (14). Then, using Eq. (12) we obtain the first of the desired equations, the $\nabla\psi$ component of Ampere's law, in the form:

$$\frac{W}{\gamma p_{0b}}\left(1+\tfrac{1}{2}\gamma\beta_b\right)=\vec{\mathbf{B}}_0\cdot\nabla\left(\frac{\xi_B}{B_0^2}\right)+\left[\nabla\cdot\left(\frac{\nabla\psi}{|\nabla\psi|^2}\right)-\frac{\beta_b}{2}\left(\frac{d\ln p_{0b}}{d\psi}+\frac{\text{æ}en_{0h}}{lp_{0b}}\right)\right]\xi_\psi+\frac{\mu_0\vec{\mathbf{J}}_{1h}\cdot\nabla\psi}{ilB_0^2}. \qquad (15)$$

To obtain the second equation, we start with background charge conservation in the form $\nabla\cdot\vec{\mathbf{J}}_{1b}=i\omega e\left(n_{1i}-n_{1e}\right)=i\omega en_{1h}$, where we also use perturbed quasi-neutrality. The expressions for the parallel and perpendicular components of the perturbed background current are calculated from the parallel component of Ampere's law and momentum equation, respectively. Using the large l approximation gives

$$\mu_0\vec{\mathbf{J}}_1\cdot\vec{\mathbf{B}}_0=\mu_0\left(\vec{\mathbf{J}}_{1b}+\vec{\mathbf{J}}_{1h}\right)\cdot\vec{\mathbf{B}}_0=\frac{1}{R^2}\nabla\psi\cdot\nabla\left(R^2Q_\zeta\right)+\frac{ilQ_\psi}{R^2}\approx+\frac{ilQ_\psi}{R^2},$$

$$\vec{\mathbf{J}}_{1b}\cdot\nabla\psi=-i\omega en_{0h}\xi_\psi+ilp_{1b}+m_in_{0i}\omega^2R^2\xi_\zeta\approx-i\omega en_{0h}\xi_\psi+ilp_{1b},$$

and

$$\vec{\mathbf{J}}_{1b}\cdot\nabla\zeta=\frac{\nabla\psi\cdot\nabla p_{1b}}{|\nabla\psi|^2}-\frac{m_in_{0i}\omega^2}{|\nabla\psi|^2}\xi_\psi-\frac{en_{0h}\omega}{l}\left(\frac{\nabla\psi\cdot\nabla\xi_\psi}{|\nabla\psi|^2}+\frac{Q_B}{B_0^2}\right)-\frac{dp_{0b}}{d\psi}\frac{Q_{B_0}}{B_0^2}.$$

Notice that we retain the inertial term in $\vec{\mathbf{J}}_{1b}\cdot\nabla\zeta$, but continue to ignore it in $\vec{\mathbf{J}}_{1b}\cdot\nabla\psi$ to be consistent with the large l expansion. Expressing p_{1b} and Q_{B_0} in terms of W and ξ_ψ, we insert the preceding three equations into the background charge conservation to obtain

$$\begin{aligned}\frac{\omega en_{1h}}{l}=\vec{\mathbf{B}}_0\cdot\nabla\left(\frac{\vec{\mathbf{B}}_0\cdot\nabla\xi_\psi}{\mu_0|\nabla\psi|^2}-\frac{\vec{\mathbf{J}}_{1h}\cdot\vec{\mathbf{B}}_0}{ilB_0^2}\right)-\left[\nabla\cdot\left(\frac{\nabla\psi}{|\nabla\psi|^2}\right)+\frac{1}{\gamma}\frac{d\ln p_{0b}}{d\psi}+\frac{\omega en_{0h}}{l\gamma p_{0b}}\right]W\\+\left(\frac{m_in_{0i}\omega^2}{R^2B_0^2}-\frac{\omega e\nabla\psi\cdot\nabla n_{0h}}{lR^2B_0^2}\right)\xi_\psi+\left(\frac{dp_{0b}}{d\psi}+\frac{\omega en_{0h}}{l}\right)\vec{\mathbf{B}}_0\cdot\nabla\left(\frac{\xi_B}{B_0^2}\right).\end{aligned} \qquad (16)$$

Finally, using the parallel component of the momentum equation to eliminate ξ_B yields

$$\vec{\mathbf{B}}_0 \cdot \nabla\left(\frac{\xi_B}{B_0^2}\right) = -\vec{\mathbf{B}}_0 \cdot \nabla\left(\frac{\vec{\mathbf{B}}_0 \cdot \nabla W}{m_i n_{0i} \omega^2 B_0^2}\right), \tag{17}$$

where we assume n_{0i} is a flux function. Substituting Eq. (17) into Eqs. (15) and (16) we now have the two coupled equations

$$-\frac{\mu_0 \vec{\mathbf{J}}_{1h} \cdot \nabla \psi}{il B_0^2} + \vec{\mathbf{B}}_0 \cdot \nabla\left(\frac{\vec{\mathbf{B}}_0 \cdot \nabla W}{m_i n_{0i} \omega^2 B_0^2}\right) = -\frac{W}{\gamma p_{0b}}\left(1 + \frac{1}{2}\gamma\beta_b\right) + \left[\nabla \cdot \left(\frac{\nabla \psi}{|\nabla \psi|^2}\right) - \frac{\beta_b}{2}\left(\frac{d \ln p_{0b}}{d\psi} + \frac{\omega \varepsilon n_{0h}}{l p_{0b}}\right)\right]\xi_\psi \tag{18}$$

and

$$\begin{aligned} &\frac{n_{1h} T_e}{p_{0b}} + \left(-\frac{l T_e}{\omega \varepsilon p_{0b}} \frac{m_i n_{0i} \omega^2}{B_0^2 R^2} + \frac{n_{0h} T_e}{p_{0b}} \frac{\nabla \psi \cdot \nabla \ln n_{0h}}{|\nabla \psi|^2}\right)\xi_\psi = -\frac{W}{\gamma p_{0b}}\left\{\frac{l T_e}{\omega \varepsilon}\left[\frac{d \ln p_{0b}}{d\psi} + \gamma \nabla \cdot \left(\frac{\nabla \psi}{|\nabla \psi|^2}\right)\right] + \frac{n_{0h} T_e}{p_{0b}}\right\} + \\ &-\left(\frac{l T_e}{\omega \varepsilon} \frac{d \ln p_{0b}}{d\psi} + \frac{n_{0h} T_e}{p_{0b}}\right)\vec{\mathbf{B}}_0 \cdot \nabla\left(\frac{\vec{\mathbf{B}}_0 \cdot \nabla W}{m_i n_{0i} \omega^2 B_0^2}\right) + \frac{l T_e}{\omega \varepsilon p_{0b}} \vec{\mathbf{B}}_0 \cdot \nabla\left(\frac{\vec{\mathbf{B}}_0 \cdot \nabla \xi_\psi}{\mu_0 |\nabla \psi|^2} - \frac{\vec{\mathbf{J}}_{1h} \cdot \vec{\mathbf{B}}_0}{il B_0^2}\right), \end{aligned} \tag{19}$$

where the terms with n_{0h} are due to the charge uncovering effect of the hot electrons on quasi-neutrality.

Observe that without hot electrons we can easily recover the well known ballooning equation for shear Alfven modes[3]. It can be obtained by substituting Eq. (18) and its poloidal flux surface average into Eq. (19) to first eliminate $\vec{\mathbf{B}}_0 \cdot \nabla W$ and then the W terms, respectively:

$$B_0^2 R^2 \vec{\mathbf{B}}_0 \cdot \nabla\left(\frac{\vec{\mathbf{B}}_0 \cdot \nabla \xi_\psi}{\mu_0 |\nabla \psi|^2}\right) + \xi_\psi\left(2\vec{\boldsymbol{\kappa}} \cdot \nabla p_{0b} + m_i n_{0i} \omega^2\right) = 4\gamma p_{0b}\left(\vec{\boldsymbol{\kappa}} \cdot \nabla \psi\right) \frac{\left\langle \xi_\psi \vec{\boldsymbol{\kappa}} \cdot \nabla \psi / B_0^2 R^2 \right\rangle}{\left(1 + \frac{1}{2}\gamma \langle \beta_b \rangle\right)}.$$

In addition to using Eq. (2) to get the right hand side of the preceding equation, we note that it follows from Eq. (18) that the variations of W along the unperturbed magnetic field are proportional to ω^2. As a result, W tends to flux function as the growth rate diminishes. In particular, from the field line average of Eq. (18)

$$W \approx -2\gamma p_{0b} \frac{\left\langle \xi_\psi \vec{\kappa}\cdot\nabla\psi / B_0^2 R^2 \right\rangle}{\left(1+\frac{1}{2}\gamma\langle\beta_b\rangle\right)},$$

where the flux surface average is defined by $\langle\ldots\rangle = V^{-1}\oint(\ldots)d\theta/\vec{\mathbf{B}}_0\cdot\nabla\theta$ with θ the poloidal angle and $V = \oint d\theta/\vec{\mathbf{B}}_0\cdot\nabla\theta$.

III. KINETIC TREATMENT OF THE HOT ELECTRONS

In the previous section we have obtained two coupled equations for quasineutrality and Ampere's law that require knowledge of the perturbed hot electron density and current. Generalizing the Z-pinch procedure developed in reference[9] to dipole geometry, we will first kinetically evaluate the perturbed hot electron responses in this section to obtain the dispersion relation in the next section. We assume that the temperature of the hot electron population, T_h, is much larger that the background temperatures, which requires that the magnetic drift and diamagnetic frequencies of the hot electrons to be much larger than the corresponding background frequencies.

We assume that the hot electrons satisfy the Vlasov equation, and following the standard procedure for solving the gyro-kinetic equation[10,11] we linearize the hot electron distribution function around the equilibrium by writing $f_h = f_{0h} + f_{1h} + \ldots$. Employing the orderings

$$\Omega_e \geq \omega_b >> \omega_{dh} \sim \omega_{*h} >> \omega, \tag{20}$$

with m the electron mass, $\Omega_e = eB_0/m$ the cyclotron frequency, $\omega_b \sim \vec{\mathbf{v}}_{||}\cdot\nabla$ the bounce frequency, and ω_{dh} and ω_{*h} the magnetic and diamagnetic frequencies, the equilibrium distribution function satisfies

$$\vec{\mathbf{v}}\cdot\nabla f_{0h}-\Omega_e\vec{\mathbf{v}}\times\hat{\mathbf{b}}\cdot\nabla_{\mathrm{v}} f_{0h}=\vec{\mathbf{v}}\cdot\nabla f_{0h}+\Omega_e\frac{\partial f_{0h}}{\partial\phi}=0\,, \tag{21}$$

where ϕ is gyrophase. As in the case of all axisymmetric machines, the toroidal component of canonical angular momentum is a constant of the motion and therefore it is useful to introduce $\psi_*=\psi-\frac{mR}{e}\hat{\boldsymbol{\zeta}}\cdot\vec{\mathbf{v}}$. Then exact solutions to Eq. (21) exist of the form $f_{0h}=f_{0h}\left(E,\psi_*\right)$, with $E=\mathrm{v}^2/2$.

To evaluate the first order correction to the hot electron distribution function we again look for solutions of the form $e^{-i\omega t-il\zeta}$ and solve the linearized Vlasov kinetic equation

$$\frac{\partial f_{1h}}{\partial t}+\vec{\mathbf{v}}\cdot\nabla f_{1h}-\Omega_e\vec{\mathbf{v}}\times\hat{\mathbf{b}}\cdot\nabla_{\mathrm{v}} f_{1h}+\frac{e}{m}\left(\nabla\Phi+\frac{\partial\vec{\mathbf{A}}}{\partial t}-\vec{\mathbf{v}}\times\vec{\mathbf{B}}_1\right)\cdot\nabla_{\mathrm{v}} f_{0h}=0\,, \tag{22}$$

where the scalar and vector potentials Φ and $\vec{\mathbf{A}}=A_{\|}\hat{\mathbf{b}}+A_{\psi}\nabla\psi/RB_0+A_{\zeta}R\nabla\zeta$, enter $\vec{\mathbf{E}}_1=-\nabla\Phi-\partial\vec{\mathbf{A}}/\partial t$ and $\vec{\mathbf{B}}_1=\nabla\times\vec{\mathbf{A}}$, with $\nabla\cdot\vec{\mathbf{A}}=0$ for the Coulomb gauge. Observe that the gauge condition coupled with the large mode number assumption causes the toroidal component of the vector potential to be small compared with the other two components: $A_{\zeta}\sim\left(A_{\psi}\ or\ A_{\|}\right)/l$.

The solution to Eq. (22) is found by removing the adiabatic piece by writing

$$f_{1h}=\frac{e\Phi}{T_h}f_{0h}+g_1\,, \tag{23}$$

and then defining $g_1=\bar{g}_1+\tilde{g}_1$ with the bar and tildes indicating the gyrophase independent and dependent parts, respectively. Using v, magnetic moment $\mu=\mathrm{v}_{\perp}^2/2B_0$, and ϕ as the velocity space variables, the resulting lowest order expressions for $\bar{g}_1$ and $\tilde{g}_1$ are given by

$$\bar{g}_1=-\frac{f_{Mh}\left(\omega-\omega_{*h}^T\right)}{\left(\omega-\frac{m\mathrm{v}^2}{2T_h}\omega_D\right)}\left(\frac{e}{T_h}\frac{\oint d\tau\left(\Phi-\mathrm{v}_{\|}A_{\|}\right)}{\oint d\tau}-\frac{m\mu}{T_h}\frac{\oint d\tau Q_B/B_0}{\oint d\tau}\right) \tag{24}$$

and

$$\tilde{g}_1 = -\Omega_e^{-1}\vec{\mathbf{v}}_\perp \times \hat{\mathbf{b}} \cdot \left[\nabla \bar{g}_1 + \frac{ie\omega}{T_h} f_{Mh}\vec{\mathbf{A}} - \frac{Q_B}{B_0^2}\frac{\partial f_{Mh}}{\partial \psi}\nabla\psi \right], \tag{25}$$

where the parallel and perpendicular subscripts refer to the components parallel and perpendicular to the equilibrium magnetic field $\vec{\mathbf{B}}_0$. The details of the calculation are given in the Appendix A. For simplicity we consider the unperturbed hot electron distribution function f_{0h} to be a Maxwellian to the lowest order and use a gyroradius expansion to write $f_{0h}(E,\psi_*) = f_{Mh} + (\psi_* - \psi)\partial f_{Mh}/\partial\psi + \ldots$ with $f_{Mh} = n_{0h}(m/2\pi T_h)^{3/2}\exp\left(-m\mathrm{v}^2/2T_h\right)$. The hot electron diamagnetic drift frequency is defined by

$$\omega_{*h}^T = \omega_{*h}\left[1 + \eta_h\left(\frac{m\mathrm{v}^2}{2T_h} - \frac{3}{2} \right) \right], \tag{26}$$

with $\omega_{*h} = \frac{lT_h}{e}\frac{d\ln n_{0h}}{d\psi}$ and $\eta_h = d\ln T_h / d\ln n_{0h}$. The effective trajectory averaged magnetic drift frequency is

$$\omega_D = \oint \frac{2lT_h\vec{\kappa}\cdot\nabla\psi}{eR^2B_0^2}\left[1 - \frac{B_0(1+s)}{2\bar{B}}\lambda\right]d\tau \Big/ \oint d\tau = -\frac{2lT_h}{m\mathrm{v}^2}\oint \vec{\mathbf{v}}_d\cdot\nabla\zeta d\tau \Big/ \oint d\tau, \tag{27}$$

with

$$\vec{\mathbf{v}}_d\cdot\nabla\zeta = -\frac{\mathrm{v}^2\vec{\kappa}\cdot\nabla\psi}{\Omega_e R^2 B_0}\left[1 - \frac{B_0(1+s)}{2\bar{B}}\lambda\right], \tag{28}$$

where

$$s = 1 - \frac{\nabla\psi\cdot\nabla\ln B_0}{\vec{\kappa}\cdot\nabla\psi} \tag{29}$$

measures the departure from the vacuum limit $s = 0$, $\lambda = \frac{\mathrm{v}_\perp^2}{\mathrm{v}^2}\frac{\bar{B}}{B_0} = \frac{\mu\bar{B}}{E}$ is a pitch angle variable with $\bar{B}$ being the value of B_0 at the outboard equatorial plane, and $d\tau \equiv \frac{d\theta}{\vec{\mathbf{v}}_\parallel\cdot\nabla\theta} > 0$ is the incremental time along the particles trajectory. We note that the trajectory integrals are different

for passing and trapped particles, with the former running over one full poloidal pass, while the latter runs over one complete bounce.

Ampere's law, Eq. (18), and, quasi-neutrality Eq. (19), require the hot electron density and $\nabla\psi$ component of perturbed hot electron current, which we form by integrating the distribution function over velocity space to obtain $n_{1h} = \int f_{1h} d\vec{\mathbf{v}}$ and $J_{1\psi} = -e\int \mathrm{v}_\psi f_{1h} d\vec{\mathbf{v}}$. Only the gyrophase independent part of g_1 contributes to n_{1h}, while only the gyrophase dependent part survives the integration in $J_{1\psi}$. The full details of the preceding calculations are presented in Appendix B.

From the form of f_1 it is clear that both n_{1h} and $J_{1\psi}$ involve $d\tau$ integrals, which involve poloidal trajectory averages of Φ, $A_\parallel$, and Q_B. In Z-pinch geometry[9] the interchange assumption removed poloidal variations. As a result, the perturbed number density and radial component of current were written as linear combinations of Φ and Q_B, while the parallel component of the Ampere's law resulted in a homogeneous equation for $A_\parallel$, allowing us to set it to zero. These simplifications permitted us to write quasineutrality and the radial component of Ampere's law as a set of two linearly coupled equations. In dipole geometry, the poloidal variation of B_0 and $\vec{\boldsymbol{\kappa}}$ cause quasineutrality and the $\nabla\psi$ component of Ampere's law to become a set of two coupled integro-differential equations, which without approximations can only be solved numerically.

To examine the possibility of a partially analytic solution we consider interchange modes, with $Q_\psi = \vec{\mathbf{B}}_0 \cdot \nabla\xi_\psi = 0$, making ξ_ψ a flux function. Next, we examine $\nabla\psi$ and $\nabla\zeta$ components of Ohm's law, Eq. (4),

$$\vec{\mathbf{E}}_1 \cdot \nabla \psi = -\nabla \Phi \cdot \nabla \psi + i\omega A_\psi R B_0 = i\omega \xi_\zeta R^2 B_0^2$$
$$\vec{\mathbf{E}}_1 \cdot \nabla \zeta = il\Phi / R^2 + i\omega A_\zeta / R = -i\omega \xi_\psi / R^2 .$$

We recall that from Eq. (11) $\xi_\zeta \sim \xi_\psi / R^2 B_0 l$, while from $\nabla \cdot \vec{\mathbf{A}} = 0$ we have $A_\zeta \sim A_\psi / l$. As a result, in the preceding expression for $\vec{\mathbf{E}}_1 \cdot \nabla \zeta$ we may neglect the A_ζ term as small by $1/l^2$, making

$$\Phi = -\omega \xi_\psi / l \tag{30}$$

a flux function to the required order (and allowing us to take it outside the $d\tau$ integrals). We also note that

$$A_\psi \sim \xi_\psi / lR . \tag{31}$$

For interchange modes Φ is up-down symmetric, while $A_\parallel$ is antisymmetric. As a result, for both the passing and trapped particles $\oint \mathrm{v}_\parallel A_\parallel d\tau = 0$ and $\vec{\mathbf{J}}_{1h} \cdot \vec{\mathbf{B}}_0 \propto \oint \mathrm{v}_\parallel \bar{g}_1 d\vec{\mathbf{v}} = 0$. Consequently, we may ignore $\vec{\mathbf{J}}_{1h} \cdot \vec{\mathbf{B}}_0$ and $A_\parallel$ terms in Eqs. (18), (19), and (24). In addition, upon gyroaveraging, the Q_B term in Eq. (25) does not survive to enter $\vec{\mathbf{J}}_{1h} \cdot \nabla \psi$ and the A_ζ component that does enter is small by $1/l^2$ as shown in Appendix B.

The last complication in Eqs. (24) and (25) is the trajectory averaged terms involving Q_B. If we combine Eqs. (12), (17) and (18) to eliminate terms involving $\vec{\mathbf{B}}_0 \cdot \nabla$ we get

$$\frac{Q_B}{\mu_0} = -\frac{\vec{\mathbf{J}}_{1h} \cdot \nabla \psi}{il} + W + \left(\frac{dp_{0b}}{d\psi} + \frac{\omega e n_{0h}}{l} \right) \xi_\psi . \tag{32}$$

For ideal MHD interchange modes near marginality both ξ_ψ and W are flux functions, so we see from Eq. (32) that in the absence of hot electrons, Q_B is also a flux function. Therefore, near marginality any variations of Q_B along the equilibrium magnetic field are caused by $\nabla \psi$

component of the hot electron current. In general $\vec{\mathbf{J}}_{1h}\cdot\nabla\psi$ and, as a result, Q_B, W, and ξ_ψ are not flux functions, causing the quasineutrality and $\nabla\psi$ component of Ampere's law to be coupled integro-differential equations. There are several options to deal with the increased complexity. One is to solve the problem numerically, which is outside the scope of the present work and probably not the most insightful approach at this point in the development of hot electron models. The second option is to treat perturbed hot electron terms as small and introduce them perturbatively. However, from the Z-pinch geometry, we know that hot electron effects can enter on equal footing with the fluid background response and play an important role in stability analysis. The third option, and the one we will pursue here, is to simply assume that Q_B, W, Φ, and $\vec{\mathbf{J}}_{1h}\cdot\nabla\psi$ are flux functions to lowest order, which allows us to obtain a dispersion relation essentially the same as the one found for a Z-pinch[9]. This procedure allows us to recover all the results from the second option, but cannot otherwise be justified in any other rigorous fashion. However, when we consider the point dipole model in Sec. V, we will find that the behavior of I, H, F, and G as a function of poloidal angle is similar to that of B_0^{-2} as required for this assumption.

Replacing Q_B, $\vec{\mathbf{J}}_{1h}\cdot\nabla\psi$ and Φ by $\langle Q_B\rangle = \langle B_\parallel B_0\rangle$, $\langle\vec{\mathbf{J}}_{1h}\cdot\nabla\psi\rangle$, and $\langle\Phi\rangle$, and taking them outside of poloidal trajectory averages in Eq. (24). To lowest significant order, we can then write the expressions for n_{1h} and $\langle\vec{\mathbf{J}}_{1h}\cdot\nabla\psi\rangle$ as

$$\frac{n_{1h}}{n_{0h}} = \frac{e\langle\Phi\rangle}{T_h}G + \langle Q_B\rangle\langle B_0^{-2}\rangle H \tag{33}$$

and

$$\frac{\mu_0\langle\vec{\mathbf{J}}_{1h}\cdot\nabla\psi\rangle}{ilB_0^2} = -\frac{\langle\beta_h\rangle}{2}\left(\frac{e\langle\Phi\rangle}{T_h}F - \langle Q_B\rangle\langle B_0^{-2}\rangle I\right), \tag{34}$$

where $\beta_h = 2\mu_0 p_{0h}/B_0^2$ and

$$G = 1 - \frac{1}{n_{0h}}\int d\vec{\mathbf{v}}\,\frac{f_{Mh}\left(\omega - \omega_{*h}^T\right)}{\left(\omega - \frac{mv^2}{2T_h}\omega_D\right)},\; H = \frac{\left\langle B_0^{-2}\right\rangle^{-1}}{n_{0h}\overline{B}^2}\int d\vec{\mathbf{v}}\,\frac{mv^2}{2T_h}\,\frac{\lambda f_{Mh}\left(\omega - \omega_{*h}^T\right)\oint d\tau\left(\overline{B}/B_0\right)/\oint d\tau}{\left(\omega - \frac{mv^2}{2T_h}\omega_D\right)},$$
$$F = \frac{\left\langle B_0^{-2}\right\rangle^{-1}}{n_{0h}B_0\overline{B}}\int d\vec{\mathbf{v}}\,\frac{mv^2}{2T_h}\,\frac{\lambda f_{Mh}\left(\omega - \omega_{*h}^T\right)}{\left(\omega - \frac{mv^2}{2T_h}\omega_D\right)},\; I = \frac{\left\langle B_0^{-2}\right\rangle^{-2}}{n_{0h}B_0\overline{B}^3}\int d\vec{\mathbf{v}}\left(\frac{mv^2}{2T_h}\right)^2\,\frac{\lambda^2 f_{Mh}\left(\omega - \omega_{*h}^T\right)\oint d\tau\left(\overline{B}/B_0\right)/\oint d\tau}{\left(\omega - \frac{mv^2}{2T_h}\omega_D\right)}. \quad (35)$$

The details of obtaining these expressions are provided in Appendix B. Notice, that in general, the expressions for G, H, F, and I contain resonant particle effects due to the possible vanishing of the denominator. Here we consider only the intermediate frequency ordering, with the wave frequency much less than the magnetic frequency of the hot electrons, so that the ω dependence in the preceding equations only matters in determining the causal path of integration about the singularity. The vanishing of the denominator corresponds to the wave – hot electron drift resonance, which can occur when ω_D is small. This resonance is weak when only very low speed hot electrons interact with the wave (no drift reversal), and possible strong for $s > 1$ when drift reversal occurs so that many hot electrons with a specific pitch angle $\lambda_{crit} = \frac{2\overline{B}}{B_0(1+s)}$ can resonate.

IV. DISPERSION RELATION

In this section we obtain the dispersion relation by substituting the expressions for $\langle n_{1h}\rangle$ and $\left\langle \vec{\mathbf{J}}_{1h}\cdot\nabla\psi\right\rangle\left\langle B_0^{-2}\right\rangle$ given by Eqs. (33) and (34) into quasineuitrality and the $\nabla\psi$ component of Ampere's law. To annihilate terms involving $\vec{\mathbf{B}}_0\cdot\nabla$ in Eqs. (18) and (19) we flux surface

average and then assume $\Phi = \langle \Phi \rangle$, $W = \langle W \rangle$, $Q_B = \langle Q_B \rangle$, and $\vec{\mathbf{J}}_{1h} \cdot \nabla \psi = \langle \vec{\mathbf{J}}_{1h} \cdot \nabla \psi \rangle$ in undifferentiated terms, and continue to use $\oint v_{\|} A_{\|} d\tau = 0 = \vec{\mathbf{J}}_{1h} \cdot \vec{\mathbf{B}}_0$. When we use Eq. (12) to eliminate $\langle W \rangle$, the resulting two coupled equations are identical in form to those obtained for a Z-pinch[9]:

$$Q_B \left\langle B_0^{-2} \right\rangle \left(1 + \tfrac{1}{2} \gamma \langle \beta_b \rangle\right) = -\frac{\mu_0}{il} \left\langle B_0^{-2} \right\rangle \left\langle \vec{\mathbf{J}}_{1h} \cdot \nabla \psi \right\rangle + \frac{\langle \beta_b \rangle}{2} \left[\frac{\langle \omega_{de} \rangle}{\omega} (\gamma - d) - \frac{n_{0h} T_e}{p_{0b}} \right] \frac{e\Phi}{T_e} \tag{36}$$

and

$$\left\langle \frac{n_{1h} T_e}{p_{0b}} \right\rangle + \left[\langle b \rangle + \frac{\langle \omega_{de} \rangle}{\omega} \frac{n_{0h} T_e}{p_{0b}} \left(1 + \frac{d \ln n_{0h}}{d \ln V}\right) - \frac{\langle \omega_{de} \rangle^2}{\omega^2} (\gamma - d) \right] \frac{e\Phi}{T_e} = Q_B \left\langle B_0^{-2} \right\rangle \left[\frac{n_{0h} T_e}{p_{0b}} - \frac{\langle \omega_{de} \rangle}{\omega} (\gamma - d) \right], \tag{37}$$

where we define

$$d = -\frac{d \ln p_{0b}}{d \ln V}, \; \langle \omega_{de} \rangle = -\frac{l T_e}{e} \frac{d \ln V}{d \psi}, \; b = \frac{l^2 T_e}{e^2 B_0^2 R^2} \frac{m_i n_{0i} T_e}{p_{0b}},$$

and employ $\left\langle \nabla \cdot \left(\nabla \psi / |\nabla \psi|^2 \right) \right\rangle = d \ln V / d \psi$. Combining the preceding two equations with Eqs. (33) and (34) to form the dispersion relation we obtain

$$\begin{aligned} &\left[\langle b \rangle + \frac{n_{0h} T_e}{p_{0b}} \left[\frac{T_e}{T_h} \langle G \rangle + \frac{\langle \omega_{de} \rangle}{\omega} \left(1 + \frac{d \ln n_{0h}}{d \ln V}\right) \right] - \frac{\langle \omega_{de} \rangle^2}{\omega^2} (\gamma - d) \right] \left(1 + \tfrac{1}{2} \gamma \langle \beta_b \rangle + \frac{\langle \beta_h \rangle}{2} \langle I \rangle \right) + \\ &+ \frac{\langle \beta_b \rangle}{2} \left[\frac{\langle \omega_{de} \rangle}{\omega} (\gamma - d) - \frac{n_{0h} T_e}{p_{0b}} \left(1 - \langle F \rangle\right) \right] \left[\frac{\langle \omega_{de} \rangle}{\omega} (\gamma - d) - \frac{n_{0h} T_e}{p_{0b}} \left(1 - \langle H \rangle\right) \right] = 0, \end{aligned} \tag{38}$$

which is the same as the Z-pinch result[9] with the exception of flux surface and trajectory averages due to geometrical effects.

Even though, the dispersion relation looks quadratic in ω, in general, the coefficients of the above dispersion relation are not necessarily real or independent of the wave frequency due to the hot electron drift resonance with the wave. As we noted in the previous section, there are two types of resonance. A weak resonance occurs when the wave interacts with a few slow

moving hot electrons. In this case, even though the imaginary parts of the coefficients in the above dispersion relation depend on the wave frequency, they are much smaller than the real parts. As a result, this type of resonance can be examined perturbatively, which is done later in the section. Another type of resonance happens when $s>1$ and drift reversal is possible. In this case the wave interacts the hot electrons of particular pitch angles, the real and imaginary parts of the coefficients are comparable in size, and the interaction is strong and always unstable. In the remainder of this section we discuss stability assuming drift reversal does not occur.

We will not consider the high frequency regime having $\langle \omega_{dh} \rangle \sim \omega >> \langle \omega_{de} \rangle$. We simply remark that in this limit the wave frequency dependencies of $\langle G \rangle$, $\langle H \rangle$, $\langle F \rangle$, and $\langle I \rangle$ terms can no longer be ignored. Consequently, the dispersion relation given by Eq. (38) is no longer a simple quadratic and its solution has to be found numerically. In this case, a new instability can occur which is often referred to as the hot electron interchange[12].

In what follows we first consider the lowest order interchange modes in the absence of resonant hot electrons for $\omega << \langle \omega_{dh} \rangle \sim \omega_{*h}$ and then retain the hot electron drift resonance perturbatively.

A. Lowest order non-resonant modes.

To investigate the effects of hot electrons on stability for closed magnetic field lines, we first ignore any resonant effects and consider the electrostatic case. To do so we drop all the terms proportional to the background plasma, by assuming $\beta_b << \beta_h \sim 1$. The dispersion relation then reduces to

$$\left(1+\frac{\langle\beta_h\rangle}{2}\langle I\rangle\right)\left[\frac{\omega^2}{\langle\omega_{de}\rangle^2}\langle b\rangle+\frac{n_{0h}T_e}{p_{0b}}\frac{\omega}{\langle\omega_{de}\rangle}\left(1+\frac{d\ln n_{0h}}{d\ln V}\right)-(\gamma-d)\right]=0. \qquad (39)$$

The overall multiplier in front is independent of the frequency, so stability requires $(n_{0h}T_e/p_{0b})^2\left(1+\frac{d\ln n_{0h}}{d\ln V}\right)^2+4\langle b\rangle(\gamma-d)\geq 0$, as in a Z-pinch[9]. The hot electrons enter only through charge uncovering effects (proportional to n_{0h}) in this limit and these improve the well known dipole interchange stability condition[3,5] of $d<\gamma$.

For the fully electromagnetic case, we continue to ignore the resonant effects of the hot electrons so that $\langle G\rangle$, $\langle H\rangle$, $\langle F\rangle$, and $\langle I\rangle$ are real and independent of wave frequency and the dispersion relation is quadratic. For the intermediate frequency ordering with $\langle\omega_{dh}\rangle >> \omega >> \langle\omega_{de}\rangle$ it follows that $\frac{T_h}{T_e}=\frac{\langle\omega_{dh}\rangle}{\langle\omega_{de}\rangle} >> \frac{\omega}{\langle\omega_{de}\rangle}$. It is expected that during LDX operation the hot electron beta will be much larger than the background beta so it is of interest to consider $\beta_h >> \beta_b \sim 1$, which coupled with the frequency ordering allows us to take $\frac{n_{0h}T_e}{p_{0b}}\sim\frac{\langle\omega_{de}\rangle}{\omega} >> \frac{T_e}{T_h}$. In this regime, the dispersion relation is given by Eq. (38) with the $\langle G\rangle$ term ignored, and stability is determined by the sign of the discriminant. This limit will be investigated in more details for the point dipole equilibrium in Sec. V.

For completeness we also examine the case of equal hot and background pressures with $\beta_h \sim \beta_b \sim 1$. Recalling the frequency ordering, this limit requires $\frac{n_{0h}T_e}{p_{0b}}\sim\frac{T_e}{T_h} << \frac{\langle\omega_{de}\rangle}{\omega}$. The dispersion relation then reduces to

$$\frac{\omega^2}{\langle\omega_{de}\rangle^2}=\frac{(\gamma-d)\left(1+\frac{1}{2}d\langle\beta_b\rangle+\frac{\langle\beta_h\rangle}{2}\langle I\rangle\right)}{\langle b\rangle\left(1+\frac{1}{2}\gamma\langle\beta_b\rangle+\frac{\langle\beta_h\rangle}{2}\langle I\rangle\right)}, \qquad (40)$$

with stability determined by the signs of three terms on the right hand side. Section V will also investigate this limit in more detail for a point dipole, for which $\gamma > d$ always, so only sign changes in the numerator need to be considered.

B. Resonant hot electron drift effects on stability.

It is also of interest to examine how weak hot electron drift resonance effects change stability boundaries. We examine these effects by retaining the imaginary parts of $\langle G \rangle$, $\langle H \rangle$, $\langle F \rangle$, and $\langle I \rangle$. Since the imaginary parts of the hot electron coefficients are much smaller than the real ones, we may examine resonant effects perturbatively by writing $\omega = \omega_0 + \omega_1$, where $\omega_0 >> |\omega_1|$ is the zero order solution to Eq. (38) with real coefficients, and ω_1 is the small complex correction due to the hot drift resonance. Due to its small size, ω_1 cannot stabilize a zero order instability or significantly affect the stability boundary, so we only look at real solutions to the dispersion relation by considering real ω_0 and ignoring the real part of ω_1. Moreover, without drift reversal, a weak drift resonance for $l > 0$ is possible only for positive wave frequencies so we require $\omega_0 > 0$. We need only consider $l > 0$ since reality requires $-\omega^*, -l$ be a solution if ω, l is a solution.

The full details of obtaining the expressions for imaginary parts of hot electrons coefficients are provided in Appendix C. Here we note that to the required order they can be written as

$$\left\langle G_{res}\right\rangle = -\Delta\frac{2p_{0b}T_h}{n_{0h}T_e^2}\Lambda_1, \qquad \left\langle H_{res}\right\rangle = \Delta\frac{\omega_0}{\langle\omega_{de}\rangle}\frac{2p_{0b}}{n_{0h}T_e}\Lambda_2,$$
$$\left\langle F_{res}\right\rangle = \Delta\frac{\omega_0}{\langle\omega_{de}\rangle}\frac{2p_{0b}}{n_{0h}T_e}\Lambda_3 \quad \text{and} \quad \left\langle I_{res}\right\rangle = \Delta\frac{\omega_0^2}{\langle\omega_{de}\rangle^2}\frac{2p_{0b}}{p_{0h}}\Lambda_4, \tag{41}$$

with Δ defined by

$$\Delta = \frac{i\sqrt{\pi}\omega_{*h}\left(1-\frac{3}{2}\eta_h\right)}{\langle\omega_{de}\rangle}\frac{n_{0h}T_e}{2p_{0b}}\sqrt{\frac{\omega_0}{\langle\omega_{de}\rangle}}\left(\frac{T_e}{T_h}\right)^{5/2}, \tag{42}$$

and the positive geometrical coefficients defined by

$$\Lambda_1 = \tfrac{1}{2}\langle\omega_{dh}\rangle^{3/2}\left\langle\frac{B_0}{\overline{B}}\int_0^{\overline{B}/B_0}\frac{d\lambda}{\omega_D^{3/2}\sqrt{1-\lambda B_0/\overline{B}}}\right\rangle,$$
$$\Lambda_2 = \frac{\langle\omega_{dh}\rangle^{5/2}}{2\overline{B}^2\left\langle B_0^{-2}\right\rangle}\left\langle\frac{B_0}{\overline{B}}\int_0^{\overline{B}/B_0}d\lambda\frac{\lambda\oint d\tau\left(\overline{B}/B_0\right)/\oint d\tau}{\omega_D^{5/2}\sqrt{1-\lambda B_0/\overline{B}}}\right\rangle,$$
$$\Lambda_3 = \frac{\langle\omega_{dh}\rangle^{5/2}}{2\overline{B}^2\left\langle B_0^{-2}\right\rangle}\left\langle\int_0^{\overline{B}/B_0}\frac{\lambda d\lambda}{\omega_D^{5/2}\sqrt{1-\lambda B_0/\overline{B}}}\right\rangle,$$
$$\Lambda_4 = \frac{\langle\omega_{dh}\rangle^{7/2}}{2\overline{B}^4\left\langle B_0^{-2}\right\rangle^2}\int_0^{\overline{B}/B_0}d\lambda\frac{\lambda^2\oint d\tau\left(\overline{B}/B_0\right)/\oint d\tau}{\omega_D^{7/2}\sqrt{1-\lambda B_0/\overline{B}}}.$$

where $\langle\omega_{dh}\rangle = \langle\omega_{de}\rangle T_h/T_e$.

The expression for the first order complex correction for the fully electromagnetic case is quite cumbersome. To understand the procedure of obtaining ω_1, we schematically represent the general zero order dispersion relation as

$$A\frac{\omega_0^2}{\langle\omega_{de}\rangle^2} + B\frac{\omega_0}{\langle\omega_{de}\rangle} + C = 0,$$

with A, B and C are the real coefficients of corresponding powers of $\omega/\langle\omega_{de}\rangle$ in Eq. (38) and given by

$$A=\left[\langle b\rangle\left(1+\tfrac{1}{2}\gamma\langle\beta_b\rangle+\frac{\langle\beta_h\rangle}{2}\langle I\rangle\right)+\frac{\langle\beta_b\rangle}{2}\left(\frac{n_{0h}T_e}{p_{0b}}\right)^2\left(1-\langle H\rangle\right)\left(1-\langle F\rangle\right)\right]$$

$$B=\frac{n_{0h}T_e}{p_{0b}}\left[\left(1+\frac{d\ln n_{0h}}{d\ln V}\right)\left(1+\tfrac{1}{2}\gamma\langle\beta_b\rangle+\frac{\langle\beta_h\rangle}{2}\langle I\rangle\right)-\frac{\langle\beta_b\rangle}{2}(\gamma-d)\left(2-\langle H\rangle-\langle F\rangle\right)\right],$$

$$C=-(\gamma-d)\left(1+\tfrac{1}{2}d\langle\beta_b\rangle+\frac{\langle\beta_h\rangle}{2}\langle I\rangle\right),$$

where the contribution from the term involving $\langle G\rangle$ is always small by at least $T_e << T_h$.

The general zero order stability boundary is described by the real solution of the preceding equation. The expression for the first order imaginary correction can be written as

$$\frac{\omega_1}{\omega_0}=\Delta NK, \tag{43}$$

where

$$\begin{aligned}K=\kappa^2&\left[\alpha^2\ \left(1-\langle H\rangle\right)\left(1-\langle F\rangle\right)-\alpha\left(2-\langle H\rangle-\langle F\rangle\right)+1\right]\Lambda_4\\&+\kappa\left\{\alpha\left[\Lambda_2\left(1-\langle F\rangle\right)+\Lambda_3\left(1-\langle H\rangle\right)\right]-\left(\Lambda_2+\Lambda_3\right)\right\}+\Lambda_1,\end{aligned} \tag{44}$$

and

$$N=\frac{\left(1+\frac{1}{2}\gamma\langle\beta_b\rangle+\frac{1}{2}\langle\beta_h\rangle\langle I\rangle\right)}{A+\frac{\langle\omega_{de}\rangle}{2\omega_0}B} \tag{45}$$

with

$$\kappa=\frac{\langle\beta_b\rangle(\gamma-d)}{2\left(1+\frac{1}{2}\gamma\langle\beta_b\rangle+\frac{1}{2}\langle\beta_h\rangle\langle I\rangle\right)}\ \text{and}\ \alpha=\frac{\omega_0 n_{0h}T_e}{\langle\omega_{de}\rangle p_{0b}(\gamma-d)}. \tag{46}$$

The sign of the Eq. (43) determines if plasma is weakly unstable. In our Z-pinch investigation, we have extensively evaluated all possible cases and requirements for this weak resonant instability. Here we will focus on three cases: electrostatic background, electromagnetic with $\beta_h\sim\beta_b\sim 1$, and the high β_h electromagnetic case $\beta_h >> \beta_b\sim 1$ for the point dipole equilibrium.

For the electrostatic background case $\beta_b << \beta_h \sim 1$, $\kappa \approx 0$, and in the absence of drift reversal $K > 0$, with ω_0 the solution of the simplified zero order dispersion relation given by Eq. (39). Equation (39) is a quadratic with real coefficients, and for the resonant modes to be of interest it must have two real stable roots. If $d > \gamma$, then both roots are positive if $d \ln n_{0h} / d \ln V < -1$, in which case the resonance is always unstable. Both roots are negative if $d \ln n_{0h} / d \ln V > -1$, in which case there is no resonance and the plasma is stable. Therefore, if $d > \gamma$ we also require $d \ln n_{0h} / d \ln V > -1$ to be completely stable due to charge uncovering effects. If $d < \gamma$, then there is always one positive root, which permits a resonance, and the stability of the region depends only on the signs of Δ and the numerator of N. For $d < \gamma$ case stability requires

$$\left(1 + \tfrac{1}{2}\langle\beta_h\rangle\langle I\rangle\right)\left(\frac{d \ln n_{0h}}{d \ln \psi} - \frac{3}{2}\frac{d \ln T_h}{d \ln \psi}\right) \le 0, \tag{47}$$

where the sign of $\langle I \rangle$ depends on sign of $d \ln p_{0h} / d \ln \psi$ and the details of the dipole magnetic field. For the point dipole considered in the next section, the sign of $\langle I \rangle$ depends only on sign of $d \ln p_{0h} / d \ln \psi$ and the plasma beta.

If we consider the electromagnetic case, with $\beta_h \sim \beta_b \sim 1$, then the α or charge uncovering terms become negligible, N reduces to $N = 1/\langle b \rangle > 0$, all Λ_j terms are positive without the drift reversal, and the expression for K becomes

$$K = \kappa^2 \Lambda_4 - (\Lambda_2 + \Lambda_3)\kappa + \Lambda_1 = \Lambda_4\left(\kappa - \frac{\Lambda_2 + \Lambda_3}{2\Lambda_4}\right)^2 + \Lambda_1 - \frac{(\Lambda_2 + \Lambda_3)^2}{4\Lambda_4}.$$

In this limit, stability depends on the sign of ΔK. If

$$d \ln n_{0h} / d \ln \psi \le \tfrac{3}{2} d \ln T_h / d \ln \psi,$$

then a sufficient condition for stability is $\Lambda_1 \geq (\Lambda_2 + \Lambda_3)^2 / 4\Lambda_4$.

If we allow $\beta_h >> 1 \sim \beta_b$, then $\alpha \sim 1$ and the general result of Eq. (43) must be considered. A sufficient condition for stability can then be seen to be $\gamma > d$, $\left(1 + \frac{1}{2}\gamma\langle\beta_b\rangle + \frac{1}{2}\langle\beta_h\rangle\langle I\rangle\right) > 0$, $\langle F\rangle < 1$, $\langle H\rangle < 1$, and $d \ln n_{0h} / d \ln \psi \leq \frac{3}{2} d \ln T_h / \ln d\psi$. However, more detailed results require a specific dipole equilibrium. In the next section we consider this high β_h case further, as well as the situations already discussed, for the point dipole equilibrium[13]. Their point dipole model allows us to simplify the computational aspect of our analysis, while retaining enough features of the general dipole geometry to be of interest to LDX.

V. POINT DIPOLE APPLICATION.

In the previous section we derived and discussed the dispersion relation for interchange stability in general dipole geometry. Unlike the Z-Pinch, the dipole dispersion relation involves flux surface averages of various geometrical quantities, making it difficult to usefully discuss stability without numerical work and a specific dipole equilibrium. To obtain semi-analytical results we adopt the point dipole equilibrium found by writing the poloidal magnetic flux in the separable form given by

$$\psi(r,u) = \psi_0 h(u) \left(\frac{r_0}{r}\right)^a , \tag{48}$$

where $u = \cos\theta$ and $R = r\sin\theta$, with r and θ spherical coordinates and θ measured from the axis of symmetry[13]. Here, ψ_0 and r_0 are normalization constants and a is a parameter between zero and one to be determined. The spatial behavior of ψ is governed by Grad-Shafranov equation, which for the choice of Eq. (48) and

$$p(\psi) = p_0 (\psi/\psi_0)^{2+4/a} \tag{49}$$

can be rewritten as an ordinary differential equation for $h(u)$:

$$\frac{d^2h}{du^2} = -\frac{a(a+1)}{(1-u^2)}h - a(a+2)\beta h^{1+4/a}, \tag{50}$$

where $\beta = \frac{2\mu_0 p_0 r_0^4}{a^2\psi_0^2}$, with p_0 being a normalization constant. Solving the preceding equation for $h(u)$ determines the eigenvalue $a = a(\beta)$, with $a \to 1$ for $\beta \to 0$ and $a \to 0$ for $\beta \to \infty$. For this model the local beta, defined in Sec. II, is only a function of poloidal angle and is given by $\beta_0 \equiv \beta a^2 h^{4/a} / \left[\left(\frac{d\ln h}{du}\right)^2 + \frac{a^2}{1-u^2} \right]$.

Using this separable form we can express the spatial dependence of all required quantities in terms of ψ, $h(u)$, and its derivatives, and evaluate all of the flux surface and trajectory averages.

We begin by addressing the issue of drift reversal in point dipole geometry, which requires the evaluation of ω_D. Figures 1 present graphs of $-\vec{\mathbf{v}}_d \cdot \nabla\zeta\left(2lT_h/m\mathrm{v}^2\right)$, which when trajectory averaged becomes ω_D, given by Eq. (27). We plot this expression as a function of u for different values of β and λ. From the graphs we can see that the integrand can become negative. However, even at large β, the particles do not spend enough time in the regions with reversed magnetic drift to make ω_D, the effective trajectory averaged drift, negative. As a result, drift reversal is not possible in point dipole geometry.

We next proceed to the evaluation of the hot electron coefficients I, F, and H, as well as their trajectory averages entering in the dispersion relation. Figures 2 illustrate the dependencies of I, F, and H on u for different values of β, where I is normalized to

$d\ln p_{0h}/d\ln\psi$, while F and H are normalized to $d\ln n_{0h}/d\ln\psi$. As we can see from the plots, all three normalized coefficients are positive at all possible u, so their flux surface averages will also be positive, as confirmed in Fig. 3, where we plot $\langle I\rangle$, $\langle F\rangle$, and $\langle H\rangle$ as a function of β. We take $d\ln n_{0h}/d\ln\psi = 1$ and $\eta_h = 0$, so that $\langle I\rangle$, $\langle F\rangle$, and $\langle H\rangle$ are normalized to $d\ln p_{0h}/d\ln\psi$ and $d\ln n_{0h}/d\ln\psi$, respectively. As we can see from the plot, the normalized flux surface average of I is positive, and both normalized $\langle F\rangle$ and $\langle H\rangle$ are also positive as well as less than unity. It is also obvious from Fig. 3 that $\langle H\rangle \approx \langle F\rangle$, and therefore the expression for K, which describes the resonant particle effects, can be approximately written as

$$K \approx \Lambda_4\left\{\kappa\left[\alpha\left(1-\langle H\rangle\right)-1\right]+\left(\Lambda_2+\Lambda_3\right)/2\Lambda_4\right\}^2+\Lambda_1-\frac{(\Lambda_2+\Lambda_3)^2}{4\Lambda_4}.$$

As a result, only if $\Lambda_1-\left(\Lambda_2+\Lambda_3\right)^2/4\Lambda_4$ becomes negative, can K change sign, an observation we will return to, when the resonant effects of hot electrons are addressed later in the section.

Next, we turn our attention to analyzing the lowest order stability condition, which ignores the resonant particle effects and for the general case is described by the dispersion relation of Eq. (38). It is convenient to illustrate this analysis with plots of d as a function of β. To do so, we use the expression that relates the total pressure gradient to the hot and the background pressure gradients, namely

$$\frac{d\ln p}{d\ln\psi} = 2+\frac{4}{a} = \frac{\langle\beta_h\rangle}{\langle\beta_0\rangle}\frac{d\ln p_{0h}}{d\ln\psi}+\frac{\langle\beta_b\rangle}{\langle\beta_0\rangle}\frac{d\ln p_{0b}}{d\ln\psi}, \tag{51}$$

where for this point dipole model the total pressure is given by Eq. (49). Notice that if we assume equal background and hot electron pressure profiles and use $d\ln V/d\ln\psi = -\left(1+3/a\right)$, we find that lowest order stability is always satisfied since $d=\left(2a+4\right)/\left(a+3\right)<\gamma=5/3$.

For the electrostatic case with $\beta_b << \beta_h \sim 1$, Eq. (51) reduces to $2+4/a \approx d\ln p_{0h}/d\ln\psi$, which when substituted in the dispersion relation given by Eq. (39) yields

$$\left(1+\frac{\langle\beta_h\rangle}{2}\langle I\rangle\right)\left[\frac{\omega^2}{\langle\omega_{de}\rangle^2}\langle b\rangle+\frac{n_{0h}T_e}{p_{0b}}\frac{\omega}{\langle\omega_{de}\rangle}\left(1-\frac{2a+4}{a+3}\frac{1}{1+\eta_h}\right)-(\gamma-d)\right]=0,$$

where we used $d\ln V/d\ln\psi=-(1+3/a)$ and $d\ln n_{0h}/d\ln\psi=(d\ln p_{0h}/d\ln\psi)/(1+\eta_h)$. The stability boundary is described by $d\le\gamma+\frac{\left(1-\frac{2a+4}{a+3}\frac{1}{1+\eta_h}\right)^2}{4\langle b\rangle(p_{0b}/n_{0h}T_e)^2}$ and can be graphically represented as in Fig. 4, where the $\eta_h=1$ and $d=\gamma$ curves overlap. As we can see from the graph, the charge uncovering effects due to hot electrons are stabilizing, and allow achieving stability with d above γ when η_h is kept negative.

Next, we consider fully electromagnetic case with $\beta_h >> \beta_b \sim 1$, so that the total plasma pressure remains mostly contained in the hot electrons. It follows from Eq. (51) that $d\ln p/d\ln p_{0h}\approx 1$, and as a result the expression for $\langle I\rangle$, which is dependent on $d\ln p_{0h}/d\ln\psi$ is positive. In addition the expressions for $1+\frac{1}{2}\gamma\langle\beta_b\rangle+\frac{1}{2}\langle\beta_h\rangle\langle I\rangle$ and the coefficient A given before Eq. (43), with $(1-\langle H\rangle)(1-\langle F\rangle)\approx(1-\langle H\rangle)^2$ are positive. The dispersion relation for this case is given by Eq. (38) without the small $\langle G\rangle$ term. The stability boundary is illustrated in Figs. 5 where d is plotted as a function of β for different values to η_h, and where the $d=\gamma$ curve overlaps with the top solid curve with the exception of the $\eta_h=-0.8$ case. As can be seen from the graphs, stability is improved in the vicinity of $\eta_h=-1$, but otherwise is rather insensitive to changes in η_h. The $b(p_{0b}/n_{0h}T_e)^2$ parameter does not affect the stability

boundary significantly. When increased (decreased), it slightly shifts the two curves together (apart), thereby decreasing (increasing) the stability region. The graphs in Figs. 5 are only valid for $\beta \approx \beta_h >> \beta_b \sim 1$, that is above about $\beta = 5$. For lower β, the stability condition is given by Fig. 4 if $\beta_b << \beta_h \sim 1$ or will be discussed shortly for $\beta_h \sim \beta_b \sim 1$.

It is also of some interest to take the hot and background pressure gradients as equal, so that Eq. (51) reduces to $2 + 4/a = d \ln p_{0h} / d \ln \psi = d \ln p_{0b} / d \ln \psi$. For this special case $d < \gamma$ and therefore A and C as given before Eq. (43), are positive and negative, respectively. Consequently, the plasma is always stable in the absence of resonant particles effects.

For the case of $\beta_h \sim \beta_b \sim 1$ the dispersion relation is given by Eq. (40) and the total plasma pressure is split between the background and hot particles. If, for example, $\langle \beta_b \rangle = \langle \beta_h \rangle = \langle \beta_0 \rangle / 2$, then Eq. (51) reduces to $4(1 + 2/a) = d \ln p_{0h} / d \ln \psi + d \ln p_{0b} / d \ln \psi$, and it follows that

$$\frac{d \ln p_{0h}}{d \ln \psi} = 4\left(1 + \frac{2}{a}\right) - \left(1 + \frac{3}{a}\right) d \, .$$

From Eq. (40), the stability boundary is determined by the signs of three expressions: $\gamma - d$, the numerator $1 + \frac{1}{2} d \langle \beta_b \rangle + \frac{\langle \beta_h \rangle}{2} \langle I \rangle$, and the denominator $1 + \frac{1}{2} \gamma \langle \beta_b \rangle + \frac{\langle \beta_h \rangle}{2} \langle I \rangle$, that are shown in Fig. 6. Unlike the previous two cases the stability boundaries are independent of η_h. As we can see from the graph, $d < \gamma$ is expected to be the only experimentally accessible stability region, since the second stability region does not cover $\beta < 1$, depends sensitively on $\langle \beta_h \rangle / \langle \beta_b \rangle$ and does not exist in the absence of hot electrons.

Next we consider the resonant hot electron effects that determine what we refer to as the first order stability boundary. We note that these effects are weak, and therefore cannot stabilize

the lowest order instability, but can potentially destabilize the zero order stable regions. Recall that resonant particle stability is determined by the sign of ω_1 , which is given by Eq. (43), and depends on the signs of ω_0, Δ, N, and K. Since the expression for ω_0 is quadratic with real coefficients, in the stable regions it will have two real roots. Only positive roots can lead to a hot electron resonance with the wave, since otherwise the denominator in the expressions $\langle I \rangle$, $\langle F \rangle$, and $\langle H \rangle$, as given in Eq. (35), will not vanish. Consequently, stable regions with two negative real roots will remain stable due to the absence of resonance. Moreover, the lowest order stable regions with two positive roots will always become weakly unstable, regardless of the signs of Δ or K. This behavior occurs because of the denominator of N, which can be written as $A + \frac{\omega_{de}}{2\omega_0} B = \pm \frac{\omega_{de}}{2\omega_0} \sqrt{B^2 - 4AC}$. As both signs are present there will always be one unstable root. In the lowest order stable regions with one positive and one negative root, only the positive root can lead to a resonant instability, and the condition for it will then be determined by the signs of N, Δ, and K. We will first concentrate on the sign of the latter.

As we have discussed earlier in this section, the sign of K depends on the sign of $\Lambda_1 - (\Lambda_2 + \Lambda_3)^2 / 4\Lambda_4$. So we present the graph of $\Lambda_1 - (\Lambda_2 + \Lambda_3)^2 / 4\Lambda_4$ as a function of β in Fig. 7. The graph shows that this expression and, as a consequence, the expression for K, are always positive. So the condition for weak resonant stability in the regions of interest depends only on the signs of Δ and the numerator of N, which are considered next for the three different cases of beta orderings.

For the electrostatic background case of $\beta_b << \beta_h \sim 1$, first order or resonant particle stability requires

$$\frac{d\ln n_{0h}}{d\ln V} = -\frac{2(2+a)}{(a+3)(1+\eta_h)} > -1$$

if $d > \gamma$, as discussed in the previous section. This is the condition for the lowest order stable region to have two negative real roots and it is satisfied when $\eta_h < -1$ or $\eta_h > (a+1)/(a+3) > 1/3$. If $d < \gamma$, then the lowest order stable region has only one real positive root, and the first order stability is given by Eq. (47). For this beta ordering $\left(1+\frac{1}{2}\langle\beta_h\rangle\langle I\rangle\right) > 0$, so the plasma will be stable to a hot electron resonant instability if $d\ln n_{0h}/d\ln\psi \le \frac{3}{2} d\ln T_h/d\ln\psi$. This condition can also be written as $(d\ln p_{0h}/d\ln\psi)\left(1-\frac{3}{2}\eta_h\right)/(1+\eta_h) \le 0$ and is satisfied when $\eta_h < -1$ or $\eta_h > 2/3$. Thus, Fig. 4 suggests that to avoid hot electron resonance destabilization we need to avoid operation with $-1 \le \eta_h < 2/3$.

For electromagnetic case of $\beta_b \sim \beta_h \sim 1$, the zero order stability boundary is independent of η_h, and stable regions always have one positive and one negative root. Therefore, as discussed in the previous section, the resonant particle stability depends only on the sign of Δ and requires $d\ln n_{0h}/d\ln\psi \le \frac{3}{2} d\ln T_h/d\ln\psi$, which as before is satisfied when $\eta_h < -1$ or $\eta_h > 2/3$. So as in the electrostatics case, the regions of operation with $-1 \le \eta_h < 2/3$ should be avoided.

For the electromagnetic case of $\beta_h >> \beta_b \sim 1$, we recall that the coefficient A, given before Eq. (43) is always positive, and the plasma will be resonant stable in the regions with $C > 0$ and $B > 0$, where it has two real negative roots. When $C < 0$ there is only one positive

root, and the sign of Δ determines the stability, so $d\ln n_{0h}/d\ln\psi \le \frac{3}{2} d\ln T_h/d\ln\psi$ is required for stability.

In this high β_h case, unless $\eta_h \to -1$, the lowest order stability boundary very closely coincides with the $C=0$ curves. As a result, except for this special case, resonant electron stability requires $d\ln n_{0h}/d\ln\psi \le \frac{3}{2} d\ln T_h/d\ln\psi$.

For the special case of $\eta_h \to -1$, the stability condition is presented in Fig. 8, where the signs of B and C are plotted as a function of β, and we also remind readers of the lowest order stability boundaries, which are shown in faint grey. In this graph, the two solid lines bound the region with $C<0$, where the plasma is resonantly stable if $d\ln n_{0h}/d\ln\psi \le \frac{3}{2} d\ln T_h/d\ln\psi$. The region above the top solid line, but below the faint grey line has $C>0$ and $B>0$, and is always stable since the two lowest order roots are negative. The region below the bottom solid line and above the faint grey line has $C>0$ and $B<0$, and is always resonantly unstable since it has two positive roots.

We conclude this section by stressing, that keeping $d<\gamma$ and $d\ln n_{0h}/d\ln\psi \le \frac{3}{2} d\ln T_h/d\ln\psi$ is the best means of keeping the plasma stable. In special cases, these conditions can be relaxed, but more profile control is required.

VI. CONCLUSIONS

We have investigated the effects of hot electrons on the interchange stability of a plasma confined by a dipole magnetic field and have obtained the general dispersion relation for arbitrary beta. The analysis of the stability boundary is dependent on the particular details of

magnetic field, as well as the background and hot electron pressure, temperature and number density profiles. As a particular illustration of the preceding theoretical development, the dispersion relation is analyzed in detail for a point dipole equilibrium.

Our analysis indicates that it is impossible to have magnetic drift reversal in the point dipole, but it might become a concern in more general dipole geometry, in which case a strong instability would occur.

If resonant hot electron effects are neglected, we find that the general, experimentally achievable interchange stability condition normally remains close to $d < \gamma$. In a point dipole we demonstrate that this condition can be improved and d can be allowed to exceed γ either in the case of an electrostatic background by keeping η_h negative, or in the electromagnetic case with $\beta_h >> \beta_b$ by keeping η_h close to negative unity.

Hot electron drift resonant effects result in small corrections to the mode frequency that can create weak instabilities in the stable regions. Usually this weak instability can be avoided by satisfying the condition $d \ln n_{0h} / d \ln \psi \leq \frac{3}{2} d \ln T_h / d \ln \psi$.

ACKNOWLEDGMENTS:

This research was supported by the U.S. Department of Energy grant No. DE-FG02-91ER-54109 at the Plasma Science and Fusion Center of the Massachusetts Institute of Technology.

The authors are extremely grateful to Andrei Simakov (LANL) for discussions as well as computational assistance. We also greatly appreciate Jay Kesner's (MIT) interest and numerous

discussions about the applications and physical interpretations of our result to the LDX experiment.

APPENDIX A: EVALUATION OF PERTURBED HOT ELECTRON DISTRIBUTION FUNCTION.

This appendix presents the detailed evaluation of the first order correction to the perturbed hot electron distribution function. We assume that the hot electrons satisfy the Vlasov equation and linearize the hot electron distribution function about its equilibrium by taking $f_h = f_{0h} + f_{1h} + \ldots$ with $f_{0h} = f_{0h}(\psi_*, E)$ satisfying Eq. (21) and f_{1h} satisfying Eq. (22). We follow the standard gyro-kinetic procedure[10,11] by removing the adiabatic response by introducing $g_1 = f_{1h} + \frac{e\Phi}{m}\frac{\partial f_{0h}}{\partial E}$ so that

$$\frac{df_{1h}}{dt} = \frac{dg_1}{dt} - \frac{d}{dt}\left(\frac{e\Phi}{m}\frac{\partial f_{0h}}{\partial E}\right) = -\frac{e}{m}\left(\nabla\Phi + \frac{\partial\vec{\mathbf{A}}}{\partial t} - \vec{\mathbf{v}}\times\vec{\mathbf{B}}_1\right)\cdot\nabla_{\mathrm{v}} f_{0h}\,, \tag{A1}$$

where $d/dt = \partial/\partial t + \vec{\mathbf{v}}\cdot\nabla - \Omega_e\vec{\mathbf{v}}\times\vec{\mathbf{B}}_0\cdot\nabla_{\mathrm{v}}$ is unperturbed Vlasov operator. Rewriting the above kinetic equation for g_1 yields

$$\begin{aligned}\frac{dg_1}{dt} &= \frac{\partial f_{0h}}{\partial E}\frac{d}{dt}\left(\frac{e\Phi}{m}\right) - \frac{e}{m}\left(\nabla\Phi + \frac{\partial\vec{\mathbf{A}}}{\partial t} - \vec{\mathbf{v}}\times\vec{\mathbf{B}}_1\right)\cdot\nabla_{\mathrm{v}} f_{0h} = \\ &= \frac{e}{m}\frac{\partial f_{0h}}{\partial E}\left(\frac{\partial\Phi}{\partial t} - \vec{\mathbf{v}}\cdot\frac{\partial\vec{\mathbf{A}}}{\partial t}\right) + \frac{\partial f_{0h}}{\partial\psi_*}R\hat{\boldsymbol{\xi}}\cdot\left(\nabla\Phi + \frac{\partial\vec{\mathbf{A}}}{\partial t} - \vec{\mathbf{v}}\times\vec{\mathbf{B}}_1\right),\end{aligned} \tag{A2}$$

where $\frac{d}{dt}\left(\frac{\partial f_{0h}}{\partial E}\right) = 0$.

We denote the gyrophase independent and dependent portions of $g_1 = \bar{g}_1 + \tilde{g}_1$ with a bar and tilde, respectively. Next, we obtain the two equations for both parts of g_1. The equation for

$\bar{g}_1$ is obtained by gyroaveraging Eq. (A2) using $E = \mathrm{v}^2/2$, $\mu = \mathrm{v}_\perp^2/2B_0$, and ϕ gyrophase on the left side. Recalling that $\tilde{g}_1$ is gyrophase periodic yields

$$\frac{\partial \bar{g}_1}{\partial t} + \vec{\mathbf{v}}_\parallel \cdot \nabla \bar{g}_1 + \left\langle \vec{\mathbf{v}}_\perp \cdot \nabla \tilde{g}_1 \right\rangle_\phi = \frac{e}{m}\frac{\partial f_{0h}}{\partial E}\left(\frac{\partial \Phi}{\partial t} - \vec{\mathbf{v}}_\parallel \cdot \frac{\partial \vec{\mathbf{A}}}{\partial t}\right) + \frac{\partial f_{0h}}{\partial \psi_*} R\hat{\boldsymbol{\xi}} \cdot \left(\nabla \Phi + \frac{\partial \vec{\mathbf{A}}}{\partial t} - \vec{\mathbf{v}}_\parallel \times \vec{\mathbf{B}}_1\right), \quad \text{(A3)}$$

with the gyrophase average defined by $\langle \ldots \rangle_\phi = \frac{1}{2\pi}\oint \ldots d\phi$. The equation for the gyrophase dependent part, $\tilde{g}_1$, is obtained by subtracting the preceding equation from Eq. (A2) to find

$$\frac{\partial \tilde{g}_1}{\partial t} + \vec{\mathbf{v}} \cdot \nabla \tilde{g}_1 + \vec{\mathbf{v}}_\perp \cdot \nabla \bar{g}_1 - \left\langle \vec{\mathbf{v}}_\perp \cdot \nabla \tilde{g}_1 \right\rangle_\phi + \Omega_e^{-1}\frac{\partial \tilde{g}_1}{\partial \phi} = -\vec{\mathbf{v}}_\perp \cdot \left(\frac{e}{m}\frac{\partial f_{0h}}{\partial E}\frac{\partial \vec{\mathbf{A}}}{\partial t} + R\frac{\partial f_{0h}}{\partial \psi_*}\vec{\mathbf{B}}_1 \times \hat{\boldsymbol{\xi}}\right). \quad \text{(A4)}$$

Using the orderings given by Eq. (20) we can expand $g_1 = g_1^0 + g_1^1 + \ldots$ and solve these two equations order by order. As a result, g_1^0 is gyrophase independent, since to lowest order Eq. (A4) gives

$$-\Omega_e \vec{\mathbf{v}} \times \hat{\mathbf{b}} \cdot \nabla_{\mathrm{v}} g_1^0 = \Omega_e \frac{\partial \tilde{g}_1^0}{\partial \phi} = 0\,. \quad \text{(A5)}$$

In addition, Eq. (A3) to lowest order requires $\vec{\mathbf{v}}_\parallel \cdot \nabla \bar{g}_1^0 = 0$, making $\bar{g}_1^0$ also a flux function to lowest order.

The solution of Eq. (A4) to next order gives us the equation for the first order gyrophase dependent part $\tilde{g}_1^1$, which we write as

$$\tilde{g}_1^1 = -\Omega_e^{-1}\vec{\mathbf{v}}_\perp \times \hat{\mathbf{b}} \cdot \left(\nabla \bar{g}_1^0 + \frac{e}{m}\frac{\partial f_{0h}}{\partial E}\frac{\partial \vec{\mathbf{A}}}{\partial t} - \frac{B_\parallel}{B_0}\frac{\partial f_{0h}}{\partial \psi_*}\nabla \psi\right) \equiv \frac{\hat{\mathbf{b}}}{\Omega_e} \times \vec{\mathbf{v}}_\perp \cdot \vec{\mathbf{D}}\,. \quad \text{(A6)}$$

With the help of the preceding equation we can calculate $\bar{g}_1^0$ from the next order version of Eq. (A3) by gyroaveraging and observing that

$$\left\langle \vec{\mathbf{v}}_\perp \cdot \nabla \tilde{g}_1^1 \right\rangle_\phi = \left\langle \vec{\mathbf{v}}_\perp \cdot \nabla\left(\frac{\hat{\mathbf{b}}}{\Omega_e}\right) \times \vec{\mathbf{v}} \right\rangle_\phi \cdot \vec{\mathbf{D}} + \left\langle \vec{\mathbf{v}}_\perp \cdot \nabla \vec{\mathbf{D}} \times \frac{\hat{\mathbf{b}}}{\Omega_e} \cdot \vec{\mathbf{v}}_\perp \right\rangle_\phi = \vec{\mathbf{v}}_d \cdot \vec{\mathbf{D}} + \frac{\mathrm{v}_\perp^2}{2}\frac{\hat{\mathbf{b}}}{\Omega_e} \cdot \nabla \times \vec{\mathbf{D}}\,,$$

with the magnetic drift velocity given by

$$\vec{\mathbf{v}}_d = -\frac{\nabla\zeta}{\Omega_e B_0}\nabla\psi\cdot\left(\frac{\mathrm{v}_\perp^2}{2}\nabla\ln B_0 + \mathrm{v}_\parallel^2\vec{\boldsymbol{\kappa}}\right).$$

Note that neither the curvature nor ∇B_0 have a $\nabla\zeta$ component.

Multiplying Eq. (A3) by $B_0/\mathrm{v}_\parallel$ and integrating over one complete poloidal circuit for the passing and one full poloidal bounce for the trapped particles to annihilate $\vec{\mathbf{v}}_\parallel\cdot\nabla\bar{g}_1^1$ we then obtain Eq. (24).

APPENDIX B: EVALUATION OF PERTURBED HOT ELECTRON NUMBER DENSITY AND RADIAL COMPONENT OF CURRENT.

In this appendix we evaluate the perturbed hot electron number density $n_{1h} = \int f_{1h} d\vec{\mathbf{v}}$ and $\nabla\psi$ component of the current, $J_{1\psi} = -e\int \mathrm{v}_\psi f_{1h} d\vec{\mathbf{v}}$, where f_{1h} is given by Eqs. (23)-(25). It is clear that only the gyrophase independent part of g_1 contributes to n_{1h}, while only the gyrophase dependent part survives the integration in $J_{1\psi}$. Thus, the perturbed number density is given by

$$n_{1h} = \frac{e\Phi}{T_h}n_{0h} - \frac{e\Phi}{T_h}\int d\vec{\mathbf{v}}\frac{f_{Mh}\left(\omega-\omega_{*h}^T\right)}{\left(\omega-\frac{m\mathrm{v}^2}{2T_h}\omega_D\right)} + \int d\vec{\mathbf{v}}\frac{m\mathrm{v}^2}{2T_h}\frac{\lambda f_{Mh}\left(\omega-\omega_{*h}^T\right)\oint d\tau\left(Q_B/B_0\bar{B}\right)/\oint d\tau}{\left(\omega-\frac{m\mathrm{v}^2}{2T_h}\omega_D\right)}$$

where $\oint \mathrm{v}_\parallel A_\parallel d\tau = 0$ since for an interchange mode $A_\parallel$ is up-down asymmetric.

The expression for $J_{1\psi} = -e\int \mathrm{v}_\psi \tilde{g}_1 d\vec{\mathbf{v}}$ may be rewritten as

$$J_{1\psi} = -\frac{mR}{2B_0}\int \mathrm{v}_\perp^2\nabla\zeta\cdot\left(\nabla\bar{g}_1 + \frac{ie\omega}{T_h}f_{Mh}\vec{\mathbf{A}}\right)d\vec{\mathbf{v}} = \frac{im}{2B_0}\int \mathrm{v}_\perp^2\left(\frac{l}{R}\bar{g}_1 - \frac{e\omega}{T_h}f_{Mh}A_\zeta\right)d\vec{\mathbf{v}}.$$

Before proceeding further we use the estimates $\bar{g}_1 \sim f_{Mh} e\Phi / T_h$ and $A_\zeta \sim A_\psi / l$ to compare the size of the terms in $J_{1\psi}$. Recalling Eqs. (30) and (31), we see that

$$\frac{f_{Mh} A_\zeta e\omega / T_h}{l\,\bar{g}_1 / R} \sim \frac{\omega R A_\psi}{l^2 \Phi} \sim 1/l^2 << 1.$$

Hence, for high mode number l we can ignore the A_ζ term compared with the $\bar{g}_1$ contribution. Therefore, the expression for $J_{1\psi}$ reduces to

$$J_{1\psi} = -\frac{e\Phi}{T_h}\frac{iml}{2R\bar{B}}\int d\vec{\mathbf{v}}\frac{\lambda \mathrm{v}^2 f_{Mh}\left(\omega - \omega_{*h}^T\right)}{\left(\omega - \frac{m\mathrm{v}^2}{2T_h}\omega_D\right)} + \frac{im^2 l}{4T_h R\bar{B}}\int d\vec{\mathbf{v}}\frac{\lambda^2 \mathrm{v}^4 f_{Mh}\left(\omega - \omega_{*h}^T\right)\oint d\tau\left(Q_B / \bar{B}B_0\right)/\oint d\tau}{\left(\omega - \frac{m\mathrm{v}^2}{2T_h}\omega_D\right)}.$$

If we also treat Q_B as a flux function to lowest order, then it can be taken outside of the $d\tau$ integrals in the expressions for n_{1h} and $J_{1\psi}$ to obtain Eqs. (33) and (34), respectively.

APPENDIX C: EVALUATION OF IMAGINARY PARTS OF *G*, *H*, *F*, AND *I* TERMS.

This appendix presents the details of obtaining the weak hot electron drift resonance terms for the intermediate frequency regime with $\langle\omega_{dh}\rangle >> \omega >> \langle\omega_{de}\rangle$. Accounting for both signs of $\mathrm{v}_\parallel$ gives $\int d\vec{\mathbf{v}} \Rightarrow \int_0^{\bar{B}/B_0}\int_0^{\infty}\int_0^{2\pi} d\phi \mathrm{v}^2 d\mathrm{v} d\lambda \left(B_0/\bar{B}\right)/2\sqrt{1-\lambda B_0/\bar{B}}$. We can then rewrite the full expressions for G, H, F, and I given by Eq. (35) at the end of Sec. III. By evaluating the ϕ integral and defining $t = \mathrm{v}\sqrt{m/2T_h}$ we obtain

$$
\begin{aligned}
G &= 1-\frac{B_0}{\sqrt{\pi}\overline{B}}\int_0^{\overline{B}/B_0}\frac{d\lambda}{\sqrt{1-\lambda B_0/\overline{B}}}\int_0^{\infty}dte^{-t^2}t^2\,\frac{\omega-\omega_{*h}\left[1+\eta_h\left(t^2-\frac{3}{2}\right)\right]}{\omega-t^2\omega_D},\\
H &= \frac{B_0\left\langle B_0^{-2}\right\rangle^{-1}}{\sqrt{\pi}\overline{B}^3}\int_0^{\overline{B}/B_0}d\lambda\,\frac{\lambda\oint d\tau\left(\overline{B}/B_0\right)/\oint d\tau}{\sqrt{1-\lambda B_0/\overline{B}}}\int_0^{\infty}dte^{-t^2}t^4\,\frac{\omega-\omega_{*h}\left[1+\eta_h\left(t^2-\frac{3}{2}\right)\right]}{\omega-t^2\omega_D},\\
F &= \frac{\left\langle B_0^{-2}\right\rangle^{-1}}{\sqrt{\pi}\overline{B}^2}\int_0^{\overline{B}/B_0}\frac{\lambda d\lambda}{\sqrt{1-\lambda B_0/\overline{B}}}\int_0^{\infty}dte^{-t^2}t^4\,\frac{\omega-\omega_{*h}\left[1+\eta_h\left(t^2-\frac{3}{2}\right)\right]}{\omega-t^2\omega_D},\\
I &= \frac{\left\langle B_0^{-2}\right\rangle^{-2}}{\sqrt{\pi}\overline{B}^4}\int_0^{\overline{B}/B_0}d\lambda\,\frac{\lambda^2\oint d\tau\left(\overline{B}/B_0\right)/\oint d\tau}{\sqrt{1-\lambda B_0/\overline{B}}}\int_0^{\infty}dte^{-t^2}t^6\,\frac{\omega-\omega_{*h}\left[1+\eta_h\left(t^2-\frac{3}{2}\right)\right]}{\omega-t^2\omega_D}.
\end{aligned}
\tag{C1}
$$

To get the non-resonant, real parts of the expressions for G, H, F for $\omega<<\langle\omega_{dh}\rangle\sim\omega_{*h}$, we simply neglect all ω dependence in the t integrals. Then we only need to evaluate the lowest order resonant contributions in the following expressions:

$$
\begin{aligned}
G &= 1-\frac{B_0\omega_{*h}\left(1-\eta_h\right)}{2\overline{B}}\int_0^{\overline{B}/B_0}\frac{d\lambda}{\omega_D\sqrt{1-\lambda B_0/\overline{B}}}+G_{res},\\
H &= \frac{B_0\left\langle B_0^{-2}\right\rangle^{-1}\omega_{*h}}{4\overline{B}^3}\int_0^{\overline{B}/B_0}d\lambda\,\frac{\lambda\oint d\tau\left(\overline{B}/B_0\right)/\oint d\tau}{\omega_D\sqrt{1-\lambda B_0/\overline{B}}}+H_{res},\\
F &= \frac{\left\langle B_0^{-2}\right\rangle^{-1}\omega_{*h}}{4\overline{B}^2}\int_0^{\overline{B}/B_0}\frac{\lambda d\lambda}{\omega_D\sqrt{1-\lambda B_0/\overline{B}}}+F_{res},\\
I &= \frac{3\left\langle B_0^{-2}\right\rangle^{-2}\omega_{*h}\left(1+\eta_h\right)}{8\overline{B}^4}\int_0^{\overline{B}/B_0}d\lambda\,\frac{\lambda^2\oint d\tau\left(\overline{B}/B_0\right)/\oint d\tau}{\omega_D\sqrt{1-\lambda B_0/\overline{B}}}+I_{res}.
\end{aligned}
\tag{C2}
$$

To calculate the small imaginary corrections due to the weak resonance, we consider the speed integrals first and note from (C1) that they are all of the form of $\int_0^{\infty}\frac{f(t)e^{-t^2}dt}{\omega-At^2}=\int_0^{\infty}dt\,\frac{f(t)e^{-t^2}}{2A\sqrt{\omega/A}}\left(\frac{1}{\sqrt{\omega/A}-t}+\frac{1}{\sqrt{\omega/A}+t}\right)$, with f being only a function of t. The imaginary part of the preceding integral is given by $-\pi i\frac{e^{-\omega/A}f\left(\sqrt{\omega/A}\right)}{2A\sqrt{\omega/A}}$ from the calculus of residues. For the intermediate frequency ordering $\sqrt{\omega/A}<<1$, so that we can approximate the exponential by

unity and only keep the largest contribution to $f\left(\sqrt{\omega/A}\right)$. As a result, for $\omega << \langle\omega_{dh}\rangle \sim \omega_{*h}$, the weak hot electron drift resonance terms to lowest order can be written as

$$
\begin{aligned}
G_{res} &\approx -\frac{i\sqrt{\pi}\sqrt{\omega}\omega_{*h}\left(1-\frac{3}{2}\eta_h\right)B_0}{2\overline{B}} \int_0^{\overline{B}/B_0} \frac{d\lambda}{\omega_D^{3/2}\sqrt{1-\lambda B_0/\overline{B}}}, \\
H_{res} &\approx \frac{i\sqrt{\pi}\omega^{3/2}\omega_{*h}\left(1-\frac{3}{2}\eta_h\right)B_0}{2\overline{B}^3\left\langle B_0^{-2}\right\rangle} \int_0^{\overline{B}/B_0} d\lambda \frac{\lambda\oint d\tau\left(\overline{B}/B_0\right)/\oint d\tau}{\omega_D^{5/2}\sqrt{1-\lambda B_0/\overline{B}}}, \\
F_{res} &\approx \frac{i\sqrt{\pi}\omega^{3/2}\omega_{*h}\left(1-\frac{3}{2}\eta_h\right)}{2\overline{B}^2\left\langle B_0^{-2}\right\rangle} \int_0^{\overline{B}/B_0} \frac{\lambda d\lambda}{\omega_D^{5/2}\sqrt{1-\lambda B_0/\overline{B}}}, \\
I_{res} &\approx \frac{i\sqrt{\pi}\omega^{5/2}\omega_{*h}\left(1-\frac{3}{2}\eta_h\right)}{2\overline{B}^4\left\langle B_0^{-2}\right\rangle^2} \int_0^{\overline{B}/B_0} d\lambda \frac{\lambda^2\oint d\tau\left(\overline{B}/B_0\right)/\oint d\tau}{\omega_D^{7/2}\sqrt{1-\lambda B_0/\overline{B}}}.
\end{aligned}
\tag{C3}
$$

Once the above expressions are flux surface averaged, they reduce to the ones given in Eq. (41) upon using $\langle\omega_{dh}\rangle = \langle\omega_{de}\rangle T_h/T_e$.

REFERENCES

[1] A. Hasegawa, Comments on Plasma Phys. Controlled Fusion **1**, 147 (1987).

[2] J. Kesner, L. Bromberg, M. E. Mauel and D. T. Garnier, *17th IAEA Fusion Energy Conference, Yokahama, Japan, 1998 (International Atomic Energy Agency, Vienna, 1999)*, Paper IAEA-F1-CN-69-ICP/09.

[3] I. B. Bernstein, E. A. Frieman, M. D. Kruskal and R. M. Kulsrud, *Proc. Roy. Soc.* London, Ser. A **244**, 17 (1958).

[4] D. Garnier, J. Kesner, M. Mauel, Phys. Plasmas **6**, 3431 (1999).

[5] A. N. Simakov, P.J. Catto, S.I. Krasheninnikov and J. J. Ramos, Phys. Plasmas **7**, 2526 (2000).

[6] J. Kesner, A. N. Simakov, D. T. Garnier, P.J. Catto, R. J. Hastie, S.I. Krasheninnikov, M. E. Mauel, T. Sunn Pedersen and J. J. Ramos, Nucl. Fusion **41**, 301 (2001).

[7] A. Hansen, D. Garnier, J. Kesner, M. Mauel and A. Ram, in *Proceedings of the 14th Topical Conference on Radio Frequency Power in Plasmas* (AIP Conf. Proceedings No. 595), edited by S. Bernanei and F. Paoletti (American Institute of Physics, New York, 2001) p. 362.

[8] D. T. Garnier, et. al. *"Production and Study of High-Beta Plasma Confined by a Superconducting Dipole Magnet"* To be published in Phys. Plasmas in 2006.

[9] N. Krasheninnikova and P.J. Catto, Phys. Plasmas, **12**, 32101 (2005).

[10] T. M. Antonsen and B. Lane, Phys. Fluids **23**, 1205 (1980).

[11] P. J. Catto, W. M. Tang and D. E. Baldwin, Plasma Physics **23**, 639 (1981).

[12] M. J. Gerver and B. G. Lane, Phys. Fluids **29**, 2214 (1986).

[13] S. I. Krasheninnikov, P. J. Catto, and R. D. Hazeltine, Phys. Plasmas **7**, 1831 (2000).

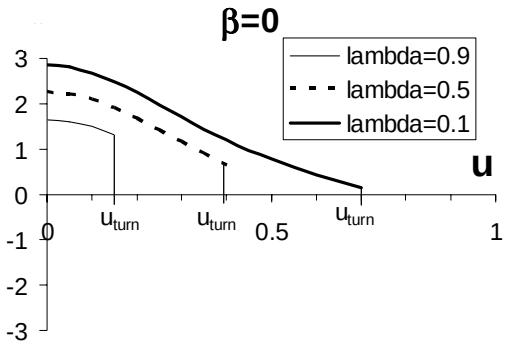

(a)

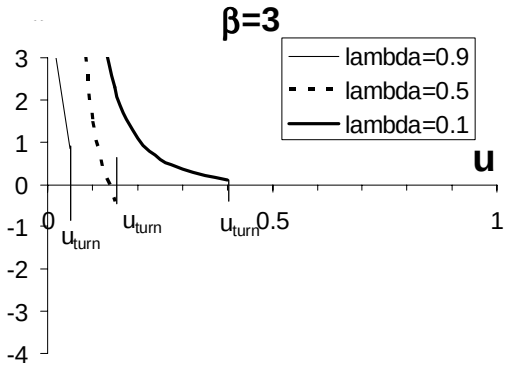

(b)

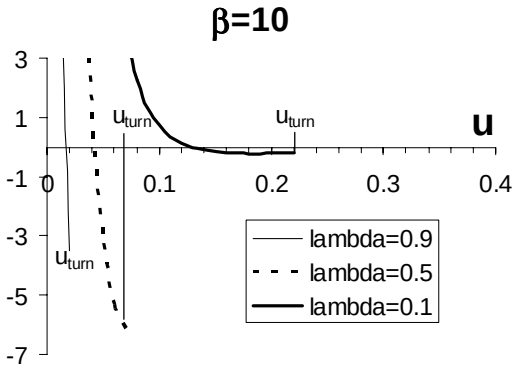

(c)

Figure 1

N.S. Krasheninnikova, P.J. Catto

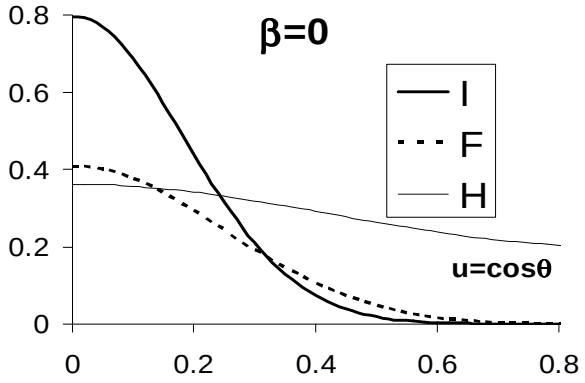

(a)

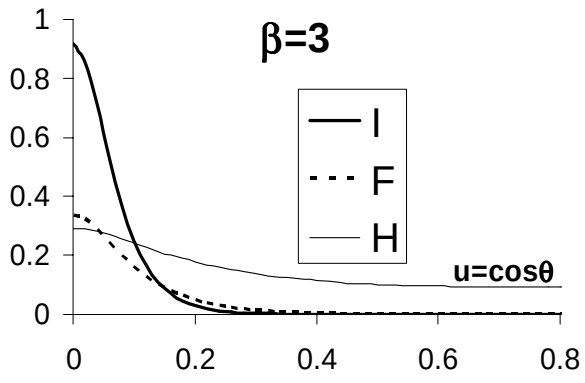

(b)

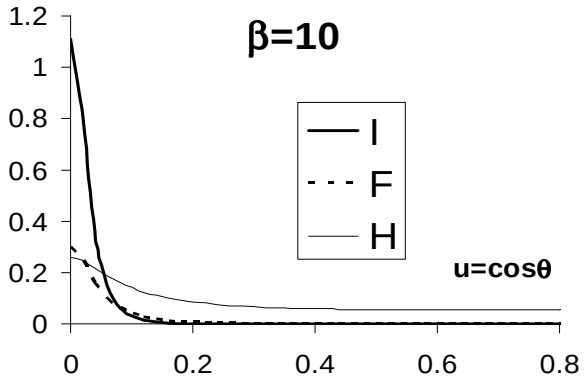

(c)

Figure 2

N.S. Krasheninnikova, P.J. Catto

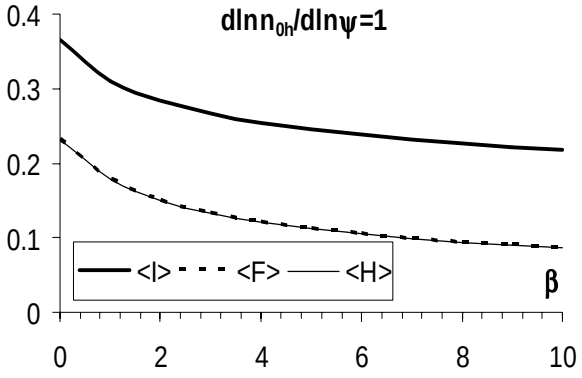

Figure 3

N.S. Krasheninnikova, P.J. Catto

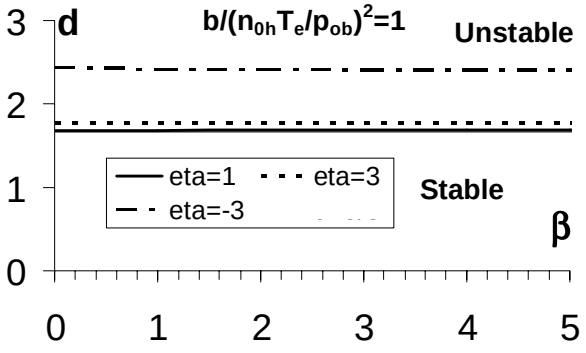

Figure 4

N.S. Krasheninnikova, P.J. Catto

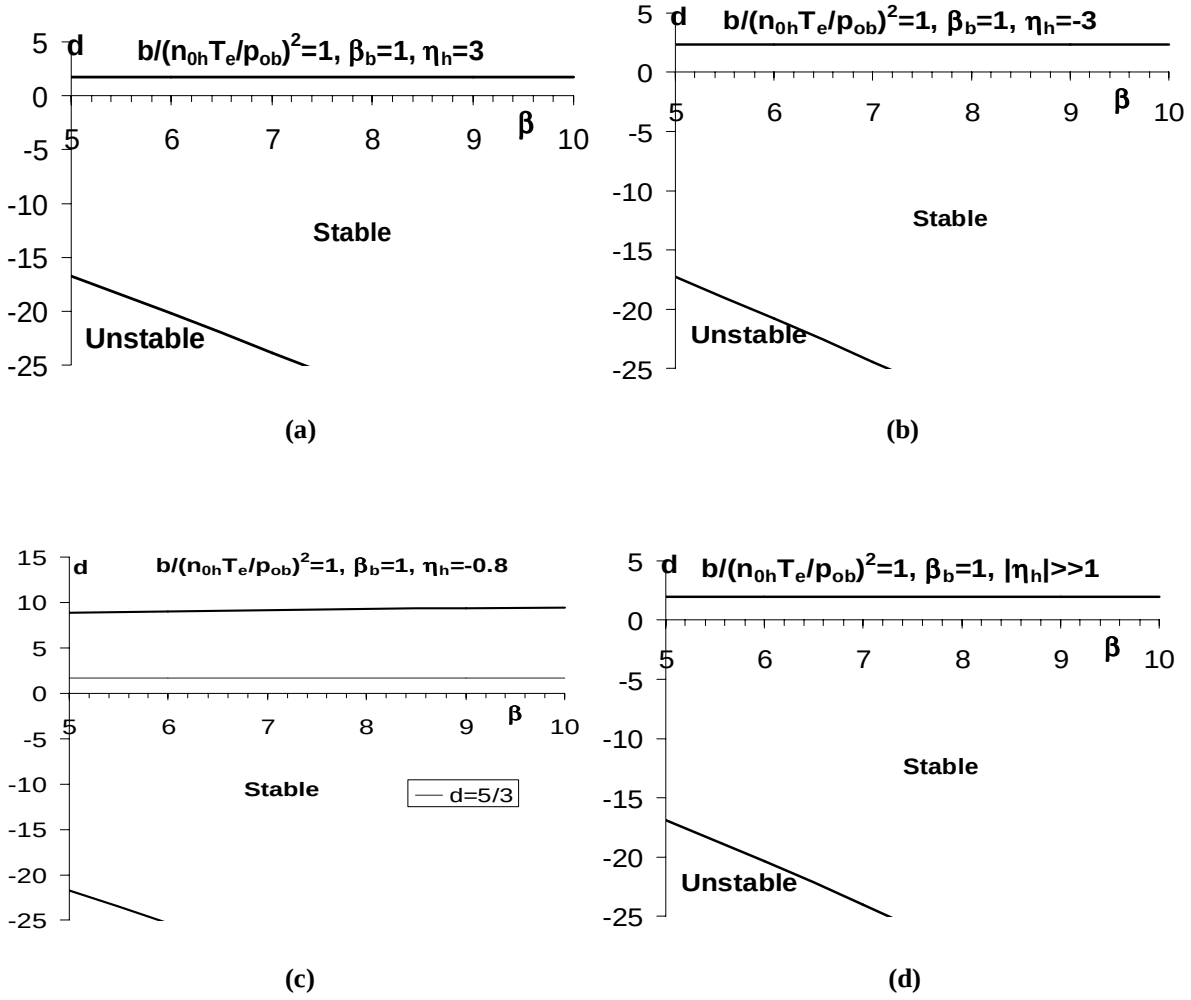

Figure 5

N.S. Krasheninnikova, P.J. Catto

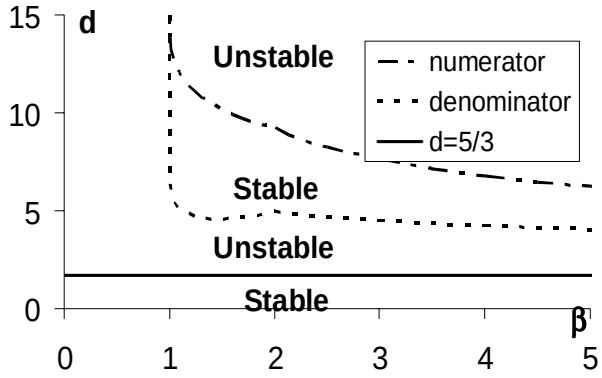

Figure 6

N.S. Krasheninnikova, P.J. Catto

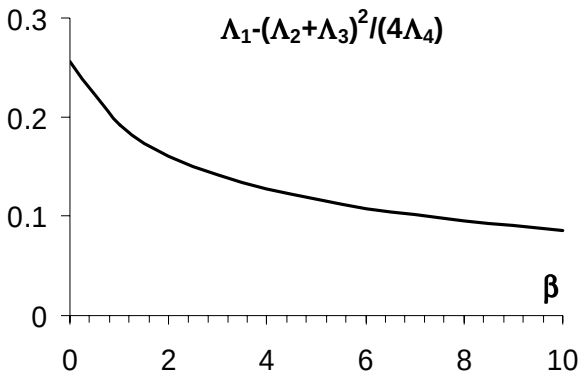

Figure 7

N.S. Krasheninnikova, P.J. Catto

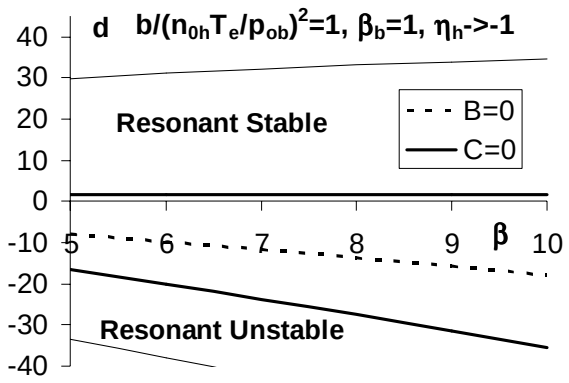

Figure 8

N.S. Krasheninnikova, P.J. Catto

FIGURE CAPTIONS

Figs. 1 (a)-(c). Expression $-\mathbf{v}_d \cdot \nabla\zeta(2lT_h/m\mathrm{v}^2)$ as a function of u for different values of β and λ. The bold solid line is λ=0.1, the thin solid line is λ=0.9, and the dotted is λ=0.5.

Figs. 2 (a)-(c). Normalized hot electron coefficients I, F, and H as a function of u for different values of β. The bold solid curve is the coefficient I, normalized to $d\ln p_{oh}/d\ln\psi$, while the dotted curve is the coefficient F and the thin solid curve is the coefficient H, both normalized to $d\ln n_{oh}/d\ln\psi$.

Figs. 3. Flux surface averages of normalized hot electron coefficients I, F, and H as a function of β with $d\ln n_{oh}/d\ln\psi$=1 and η_h=0 for normalization. The bold solid line is $\langle I\rangle$, the dotted line is $\langle F\rangle$, and the thin solid line is $\langle H\rangle$.

Figs. 4. Stability regions for different values of η_h with $b(p_{0b}/n_{0h}T_e)^2$=1. The bold solid curve is η_h =1, which coincides with the thin solid line d=γ. The dash-dotted line is η_h =-3 and the dotted line is η_h =3.

Figs. 5 (a)-(d). Stability regions for different values of η_h with β_b =1 and $b(p_{0b}/n_{0h}T_e)^2$=1. The thin solid line is d=γ. In figures (a), (b), and (d) it overlaps with the top solid curve.

Figs. 6. Stability regions for $\langle\beta_b\rangle=\langle\beta_h\rangle=\langle\beta_0\rangle/2$. The bold solid curve is d=γ, the dash-dotted line is $1+d\langle\beta_b\rangle/2+\langle I\rangle\langle\beta_h\rangle/2=0$, the dotted line is $1+\gamma\langle\beta_b\rangle/2+\langle I\rangle\langle\beta_h\rangle/2=0$.

Fig. 7 Graph of $\Lambda_1-(\Lambda_2+\Lambda_3)^2/(4\Lambda_4)$ vs. β.

Figs. 8. Stability regions for η_h–>-1 with β_b =1 and $b(p_{0b}/n_{0h}T_e)^2$=1. The dotted line is B=0, two bold solid lines are C=0 and thin solid lines are the lowest order boundaries as shown in Figs. 2.